Emerging Neuroimaging Techniques for Brain Tumor Characterization and Beyond

Presenter: Jingwen Yao

M229 Advanced Topics in MRI

May 30, 2023

Medical Imaging Modalities

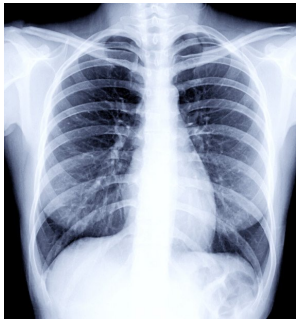

X-ray

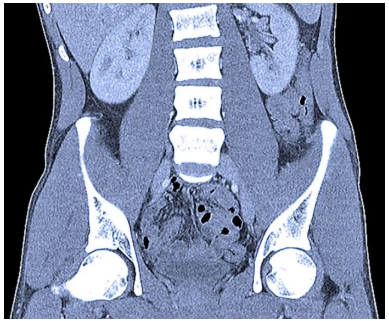

CT

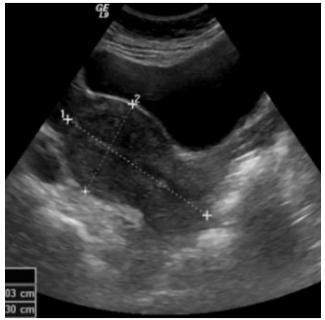

US

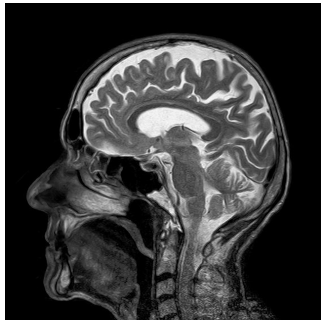

MRI

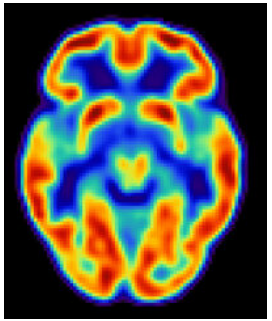

PET/SPECT

- Best for soft tissue contrast
- No ionizing radiation
- Full body multi-planar imaging
- External contrast optional

Medical Imaging Modalities

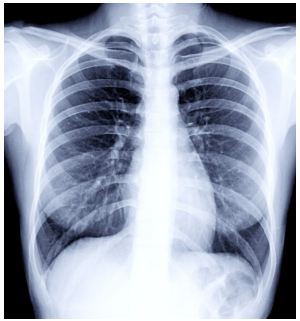

X-ray

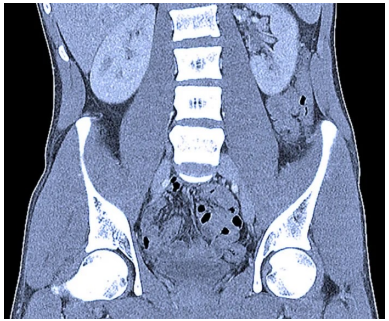

CT

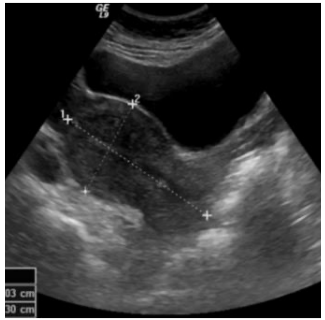

US

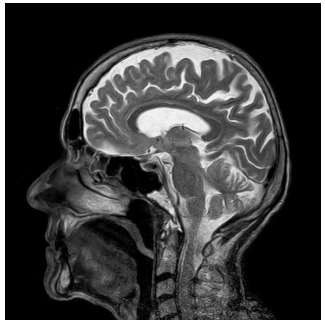

MRI

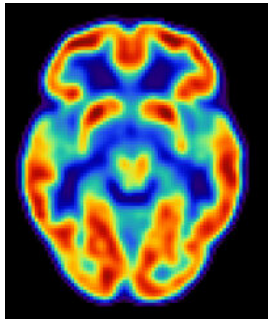

PET/SPECT

Higher spatial resolution

Lower spatial resolution

Structural information

Functional information

Magnetic Resonance Imaging

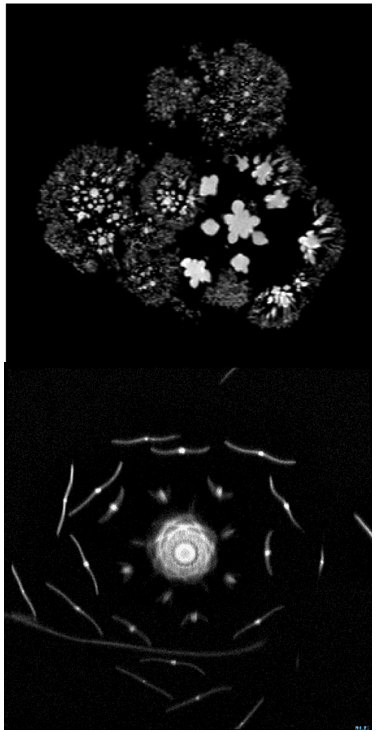

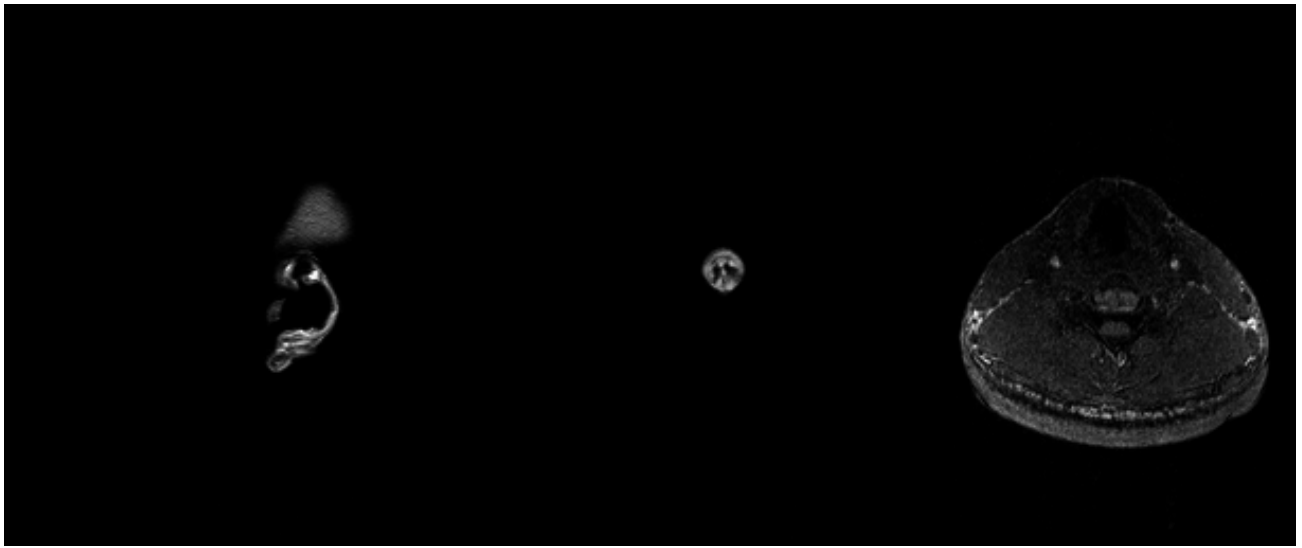

Neuroimaging

Anatomic imaging

- Structural information

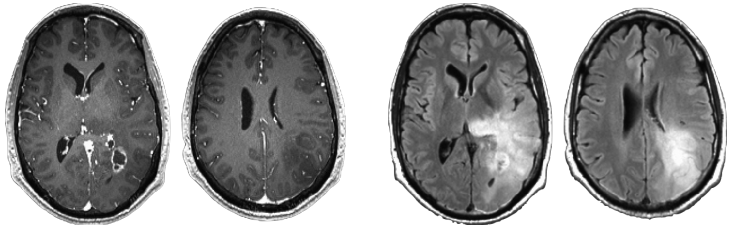

Diffusion Imaging

- Cellularity, neurite density, structural connectivity
- Surgery planning

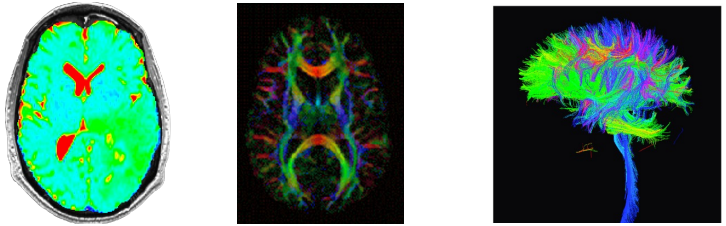

Perfusion Imaging

- Blood volume, blood flow, vessel permeability

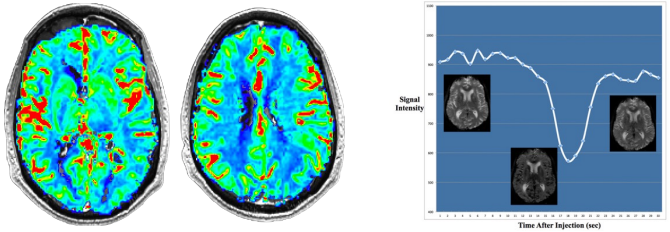

Neuroimaging

Functional MRI

- Activation map
- Functional connectivity

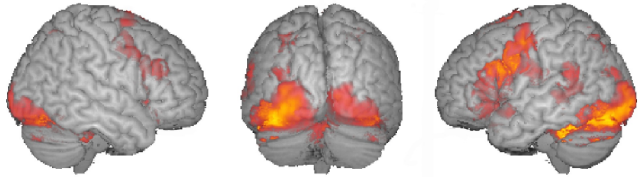

MR Spectroscopy

- Chemical composition

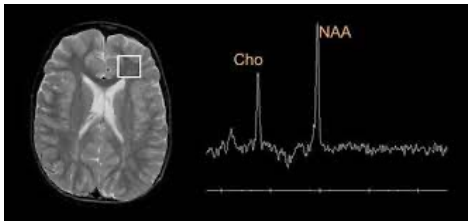

Susceptibility Imaging

- Hemorrhage, microbleed, veins, iron deposition

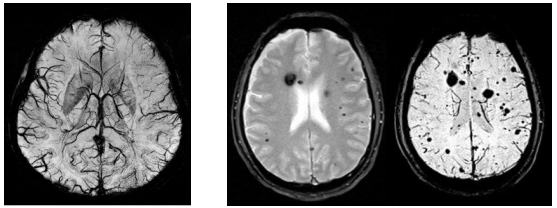

Neuroimaging

Routine clinical use

Anatomic imaging, diffusion imaging, perfusion imaging, MR angiography, etc.

Clinical niche, drug trials

Functional imaging, susceptibility imaging, MR spectroscopy, etc.

Research

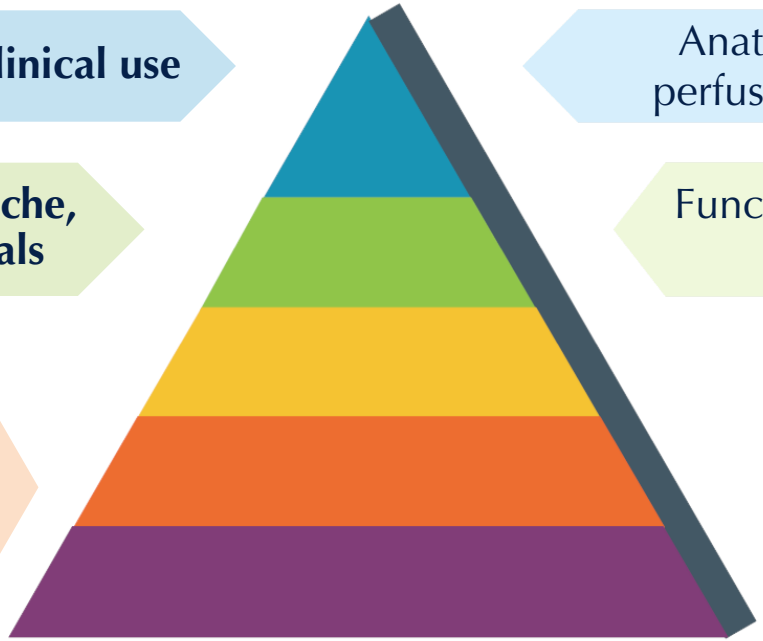

Myelin water imaging

Elastography

qMT

QSM

HP-^{13}C

ASL

X-nulei

CEST

Multicontrast MRI

Neuroimaging

Routine clinical use

Anatomic imaging, diffusion imaging, perfusion imaging, MR angiography, etc.

Clinical niche, drug trials

Functional imaging, susceptibility imaging, MR spectroscopy, etc.

Research

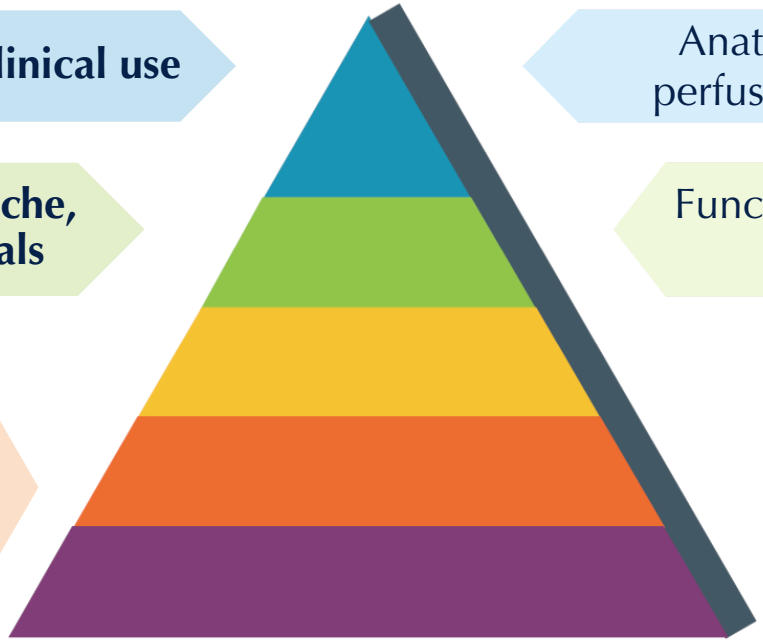

Myelin water imaging

Elastography

qMT

QSM

HP-^{13}C

ASL

X-nulei

CEST

Multicontrast MRI

Outline

CEST

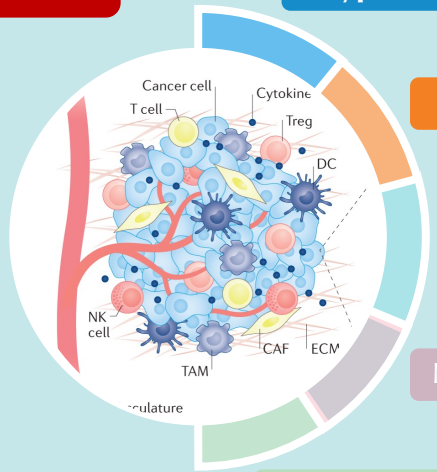

Hypoxia

Acidosis

Ion homeostasis

Neo-vasculature

Immune modulation

Glioma microenvironment

QSM

Brain iron imaging of subcortical nuclei in HD

Huntington's disease

Ongoing projects

1. Tumor associated macrophage imaging using ferumoxytol MRI
2. Understanding the role of cerebellum in HD

Glioma

Glioma

27% CNS tumors

81% malignant CNS tumors

Glioblastoma (GBM)

58% gliomas

5-year relative survival rate 7.2%

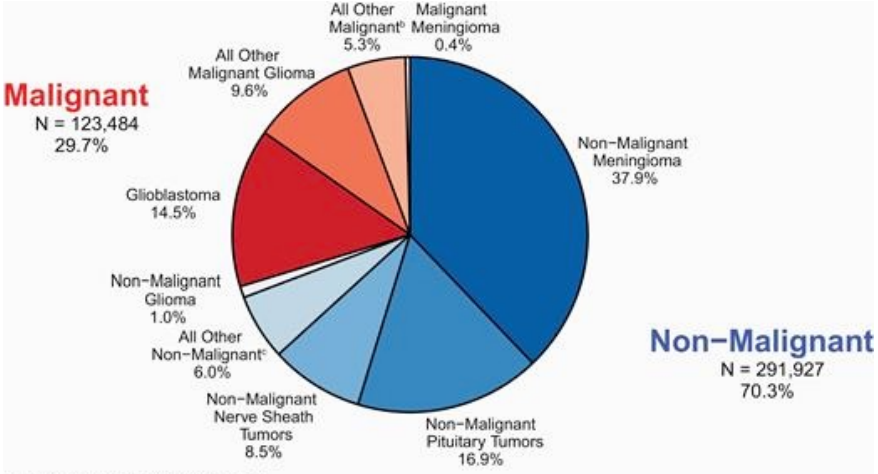

Ostrom QT et al., Neuro-Oncology, 2020

Tumor Metabolism and Microenvironment

Abnormal Vasculature

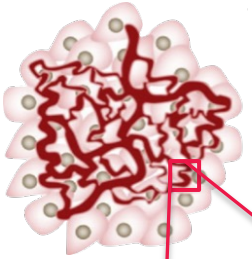

Hypoxia

Tumor Growth Away from Vasculature

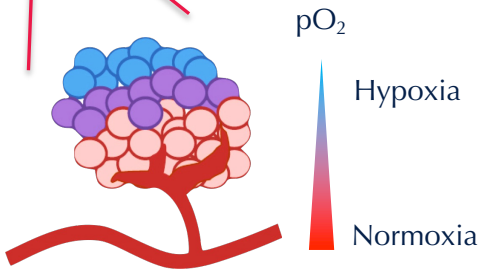

Tumor invasion
Angiogenesis
Resistance to therapy
Decreased immune function
…

Aerobic Glycolysis

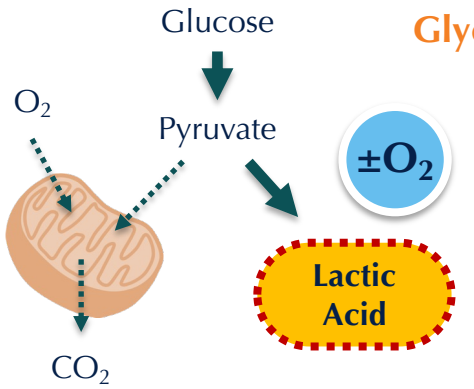

Acidity

pH- and Oxygen-Sensitive Imaging for Glioma

Technical development and validation

Sequence Design and Implementation

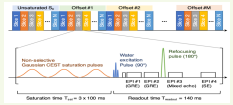

A Physical Phantom for CEST MRI

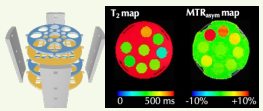

Improved B_0-Correction Algorithm

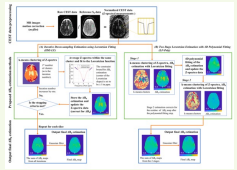

Evaluation of *in vivo* Variability

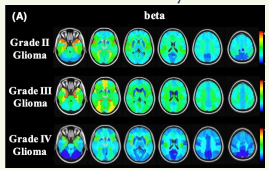

Biological validation

Correlation with Cellular Metabolomics, Tissue IHC Biomarkers, and Glioma Mice Model Tumor Burden

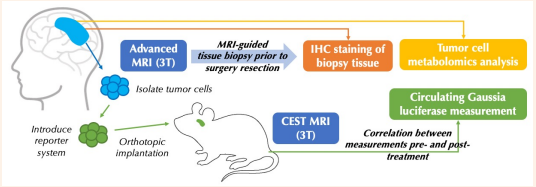

Correlation with Perfusion MRI

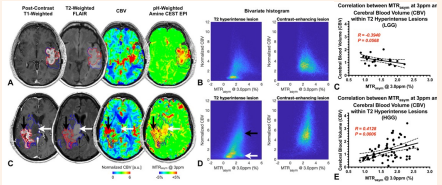

Clinical validation

Metabolic Differences across Glioma Genotypes

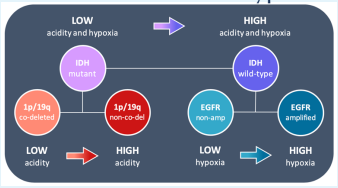

Prognostics Biomarker for Glioma Patient Survival

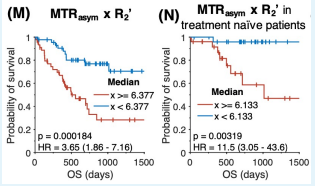

Imaging Biomarker for Treatment Efficacy Assessment

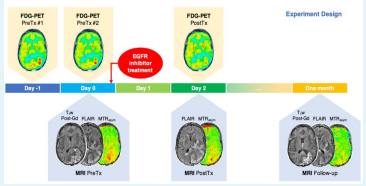

Development and validation of a pH- and oxygen-sensitive MRI technique

pH- and Oxygen-Sensitive Imaging for Glioma

Technical development and validation

Biological validation

Clinical validation

Sequence Design and Implementation

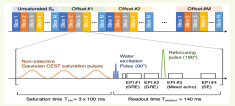

Improved B_0-Correction Algorithm

Evaluation of *in vivo* Variability

A Physical Phantom for CEST MRI

Correlation with Cellular Metabolomics, Tissue IHC Biomarkers, and Glioma Mice Model Tumor Burden

Correlation with Perfusion MRI

Metabolic Differences across Glioma Genotypes

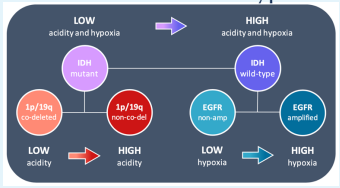

Prognostics Biomarker for Glioma Patient Survival

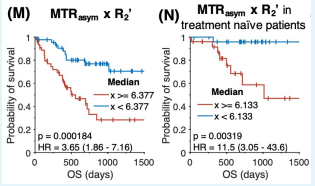

Imaging Biomarker for Treatment Efficacy Assessment

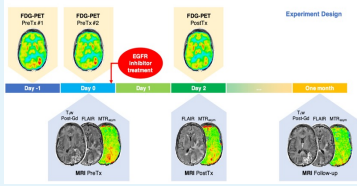

Development and validation of a pH- and oxygen-sensitive MRI technique

CEST-SAGE-EPI Sequence

CEST SAGE EPI

Chemical Exchange Saturation Transfer

Chemical Exchange Saturation Transfer

Source of MR signal

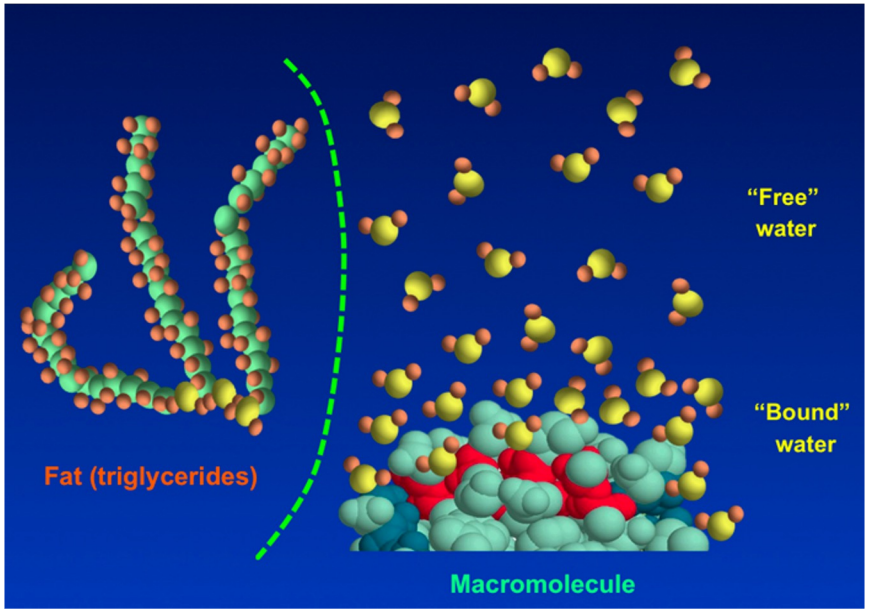

Chemical Exchange Saturation Transfer

Source of MR signal

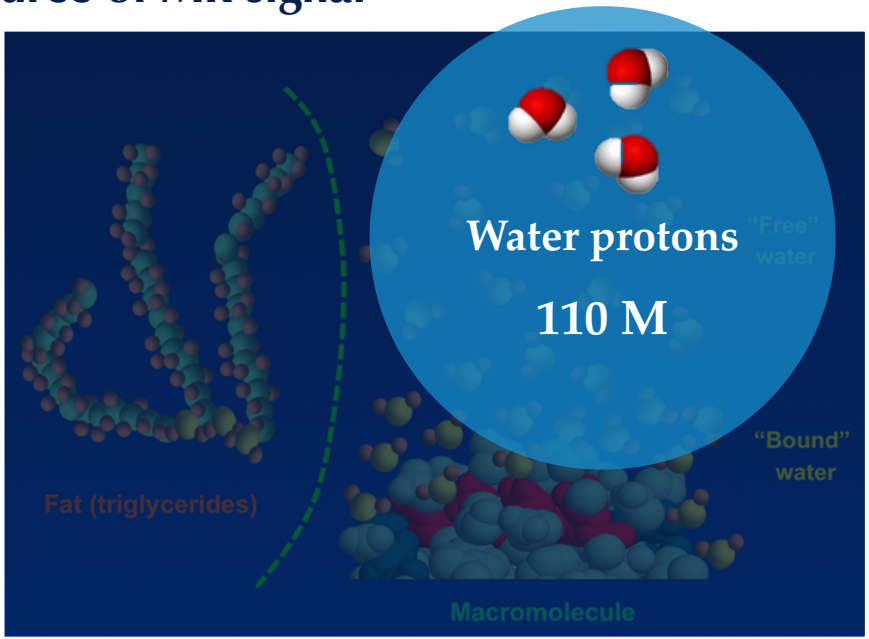

Labile molecules

uM to mM

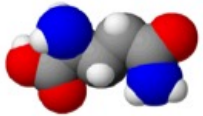

Amine: -NH_2

CEST SAGE EPI

Chemical Exchange Saturation Transfer

Labile molecules

uM to mM

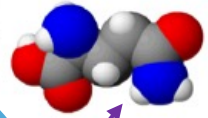

Amine: -NH_2

Chemical exchange

Water protons

110 M

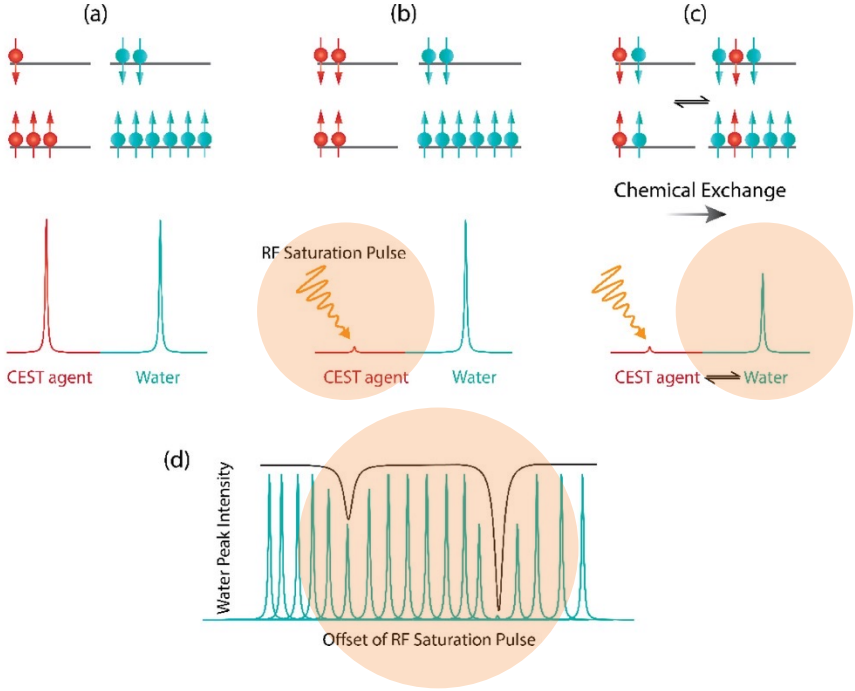

Pavuluri K et al., IJC, 2017

CEST SAGE EPI

Chemical Exchange Saturation Transfer

Labile molecules

uM to mM

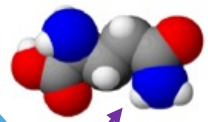

Amine: -NH_2

Chemical exchange

Water protons

110 M

Base catalyzed

$$k_b = k_0 + k_{\text{base}} * 10^{-(14-pH)}$$

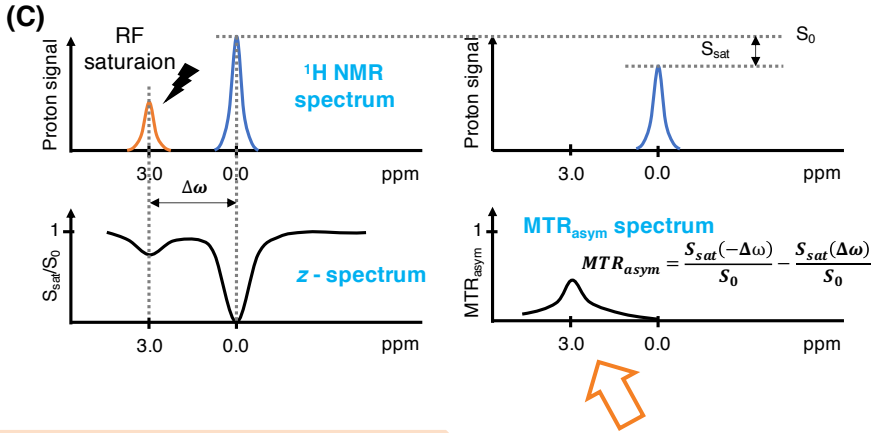

- Metabolite concentration
- Chemical exchange rate

CEST effect

CEST SAGE EPI

Chemical Exchange Saturation Transfer

Labile molecules

uM to mM

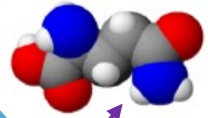

Amine: -NH_2

Chemical exchange

Base catalyzed

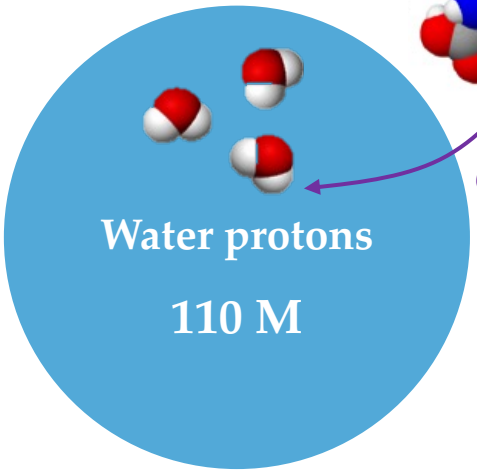

Bloch-McConnell equations

$$\frac{d\boldsymbol{M}(t)}{dt} = \boldsymbol{X} \cdot \boldsymbol{M}(t) - \boldsymbol{c},$$

$$\boldsymbol{M} = \begin{pmatrix} M_{ax} \\ M_{bx} \\ M_{ay} \\ M_{by} \\ M_{az} \\ M_{bz} \end{pmatrix}, \boldsymbol{X} = \begin{pmatrix} C_{2a} & k_b & -\delta a & 0 & 0 & 0 \\ k_a & C_{2b} & 0 & -\delta b & 0 & 0 \\ \delta a & 0 & C_{2a} & k_b & -\omega_1 & 0 \\ 0 & \delta b & k_a & C_{2b} & 0 & -\omega_1 \\ 0 & 0 & \omega_1 & 0 & C_{1a} & k_b \\ 0 & 0 & 0 & \omega_1 & k_a & C_{1b} \end{pmatrix}, \boldsymbol{c} = \begin{pmatrix} 0 \\ 0 \\ 0 \\ 0 \\ M_{az0}/T_{1a} \\ M_{bz0}/T_{1b} \end{pmatrix},$$

CEST SAGE EPI

Chemical Exchange Saturation Transfer

Labile molecules

uM to mM

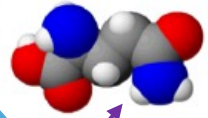

Amine: -NH_2

Chemical exchange

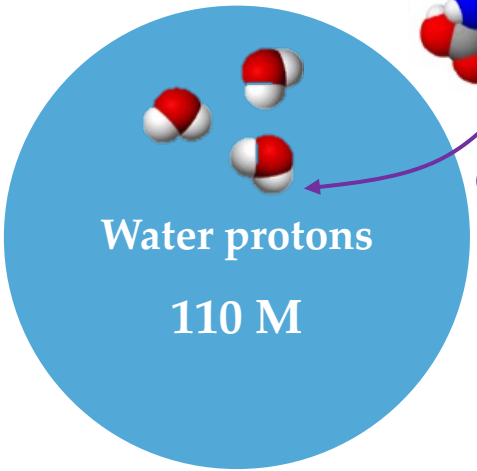

Base catalyzed

Bloch-McConnell equations

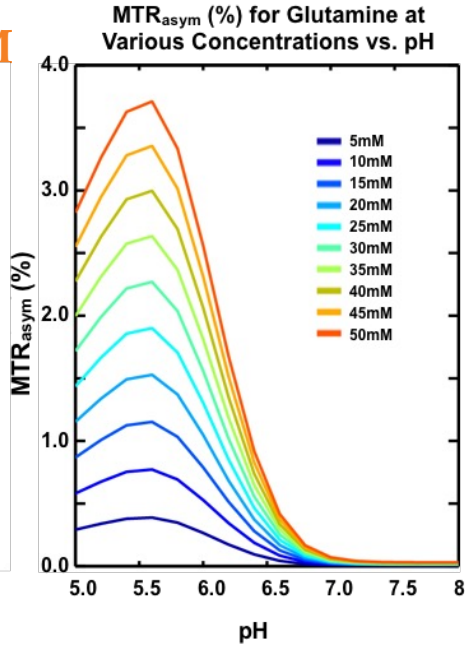

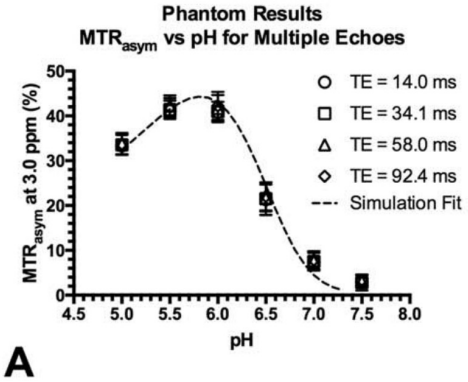

A

Harris RJ*, **Yao J***, et al., MRM, 2018

CEST SAGE EPI

Spin-And-Gradient Echo

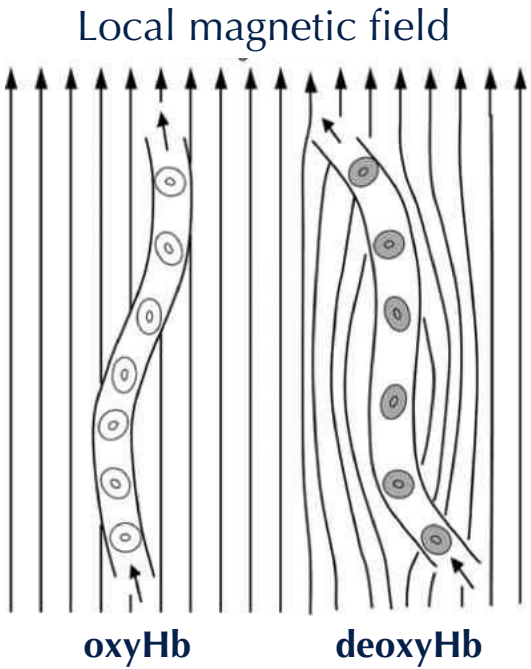

- **Blood-oxygenation level dependent (BOLD)** effect
- Reversible transverse relaxation rate R_2'

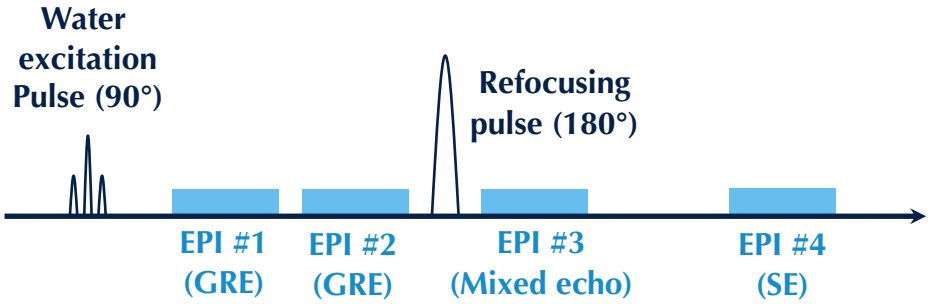

CEST SAGE EPI

Spin-And-Gradient Echo

$$A = Y^{-1}S$$

$$S = \begin{pmatrix} ln(S_1) \\ ln(S_2) \\ ln(S_3) \\ ln(S_4) \end{pmatrix}, \quad Y = \begin{pmatrix} 1 & 0 & -TE_1 & 0 \\ 1 & 0 & -TE_2 & 0 \\ 1 & -1 & -TE_4 + TE_3 & TE_4 - 2 \cdot TE_3 \\ 1 & -1 & 0 & -TE_4 \end{pmatrix}, \quad A = \begin{pmatrix} ln(S_0) \\ ln(\delta) \\ R_2^* \\ R_2 \end{pmatrix}$$

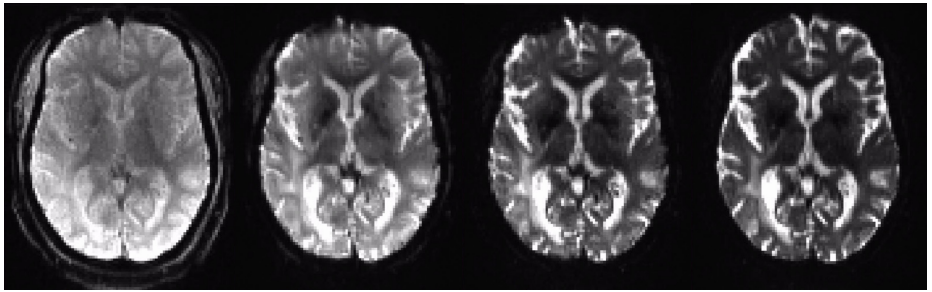

$$R_2' = R_2^* - R_2$$

$$rOEF = \frac{R_2'}{\left(\frac{4}{3}\gamma \cdot \pi \cdot \Delta\chi \cdot B_0\right) \cdot rCBV}$$

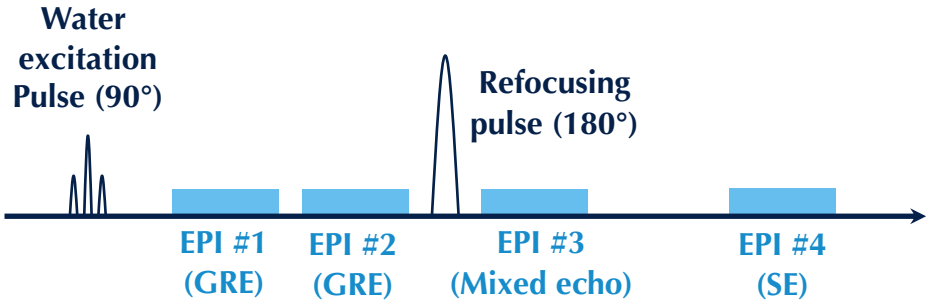

Echo-Planar Imaging

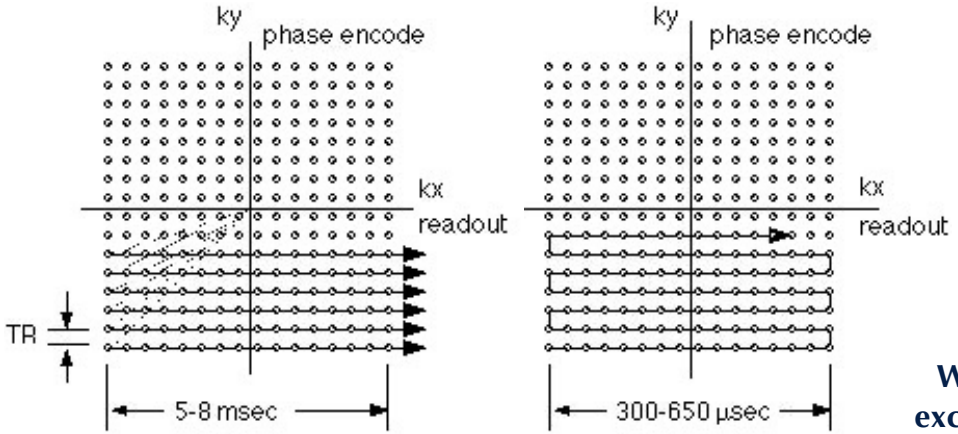

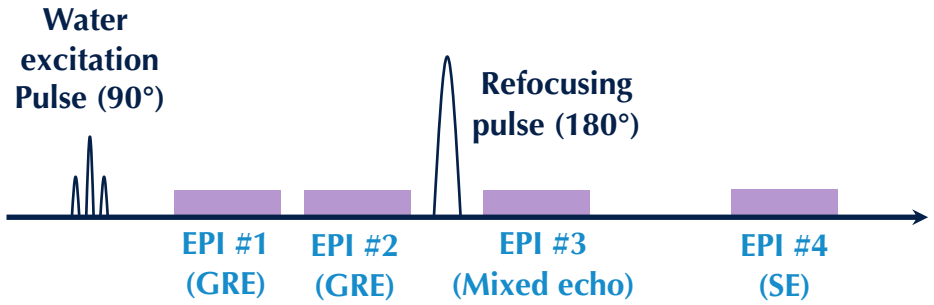

CEST-SAGE-EPI sequence

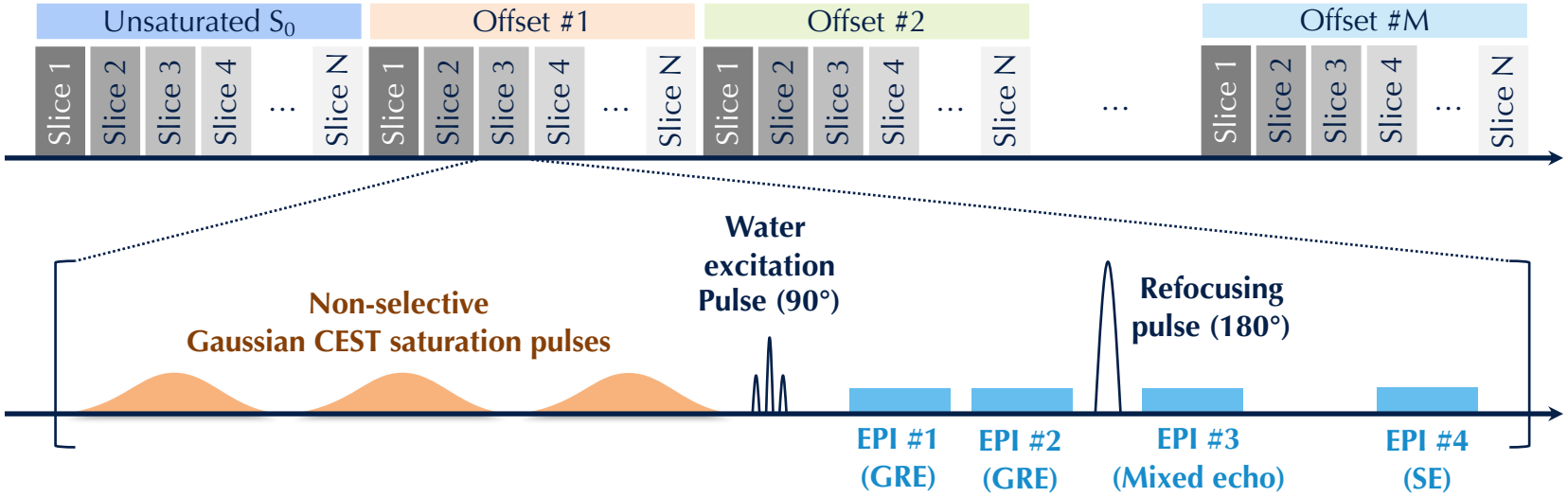

CEST pH-sensitive

SAGE-EPI Oxygen-sensitive

Harris RJ*, **Yao J***, et al., MRM, 2018

CEST-SAGE-EPI sequence

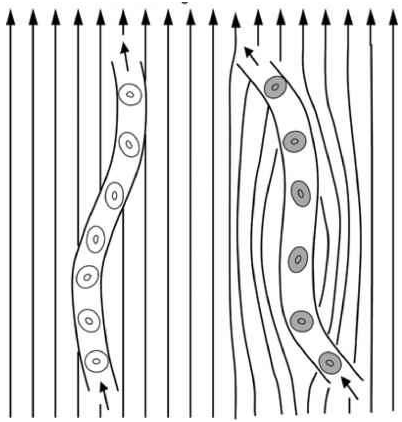

Hypoxia

Reversible transverse relaxation

$R_2' = R_2^* - R_2$

Spin-and-gradient echo (SAGE)

Higher R_2'

↓

More hypoxic

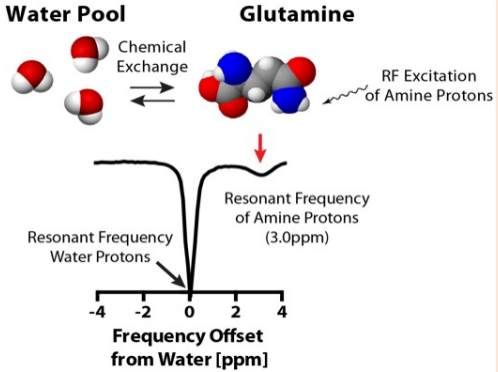

Acidity

pH-sensitive **amineCEST**

Chemical exchange saturation transfer

Higher MTR_{asym}

↓

More acidic

Harris RJ*, **Yao J***, et al., MRM, 2018

Clinical validation of pH- and oxygen-sensitive MRI

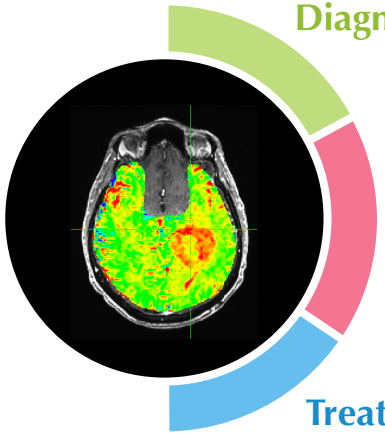

Diagnostic biomarker — Does the biomarker predict glioma genotypes?

Prognostic biomarker — Does the biomarker predict patient survival?

Treatment efficacy biomarker — Does the biomarker predict patient outcome?

Clinical validation of pH- and oxygen-sensitive MRI

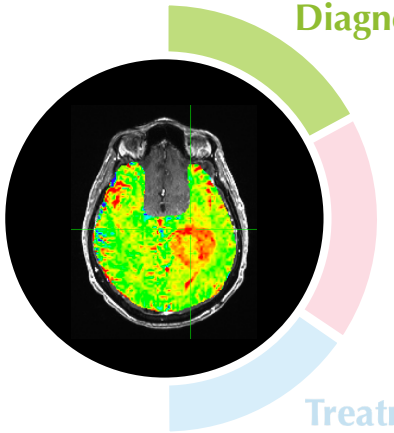

Diagnostic biomarker — Does the biomarker predict glioma genotypes?

Prognostic biomarker — Does the biomarker predict patient survival?

Treatment efficacy biomarker — Does the biomarker predict patient outcome?

Clinical validation: differentiating glioma genotypes

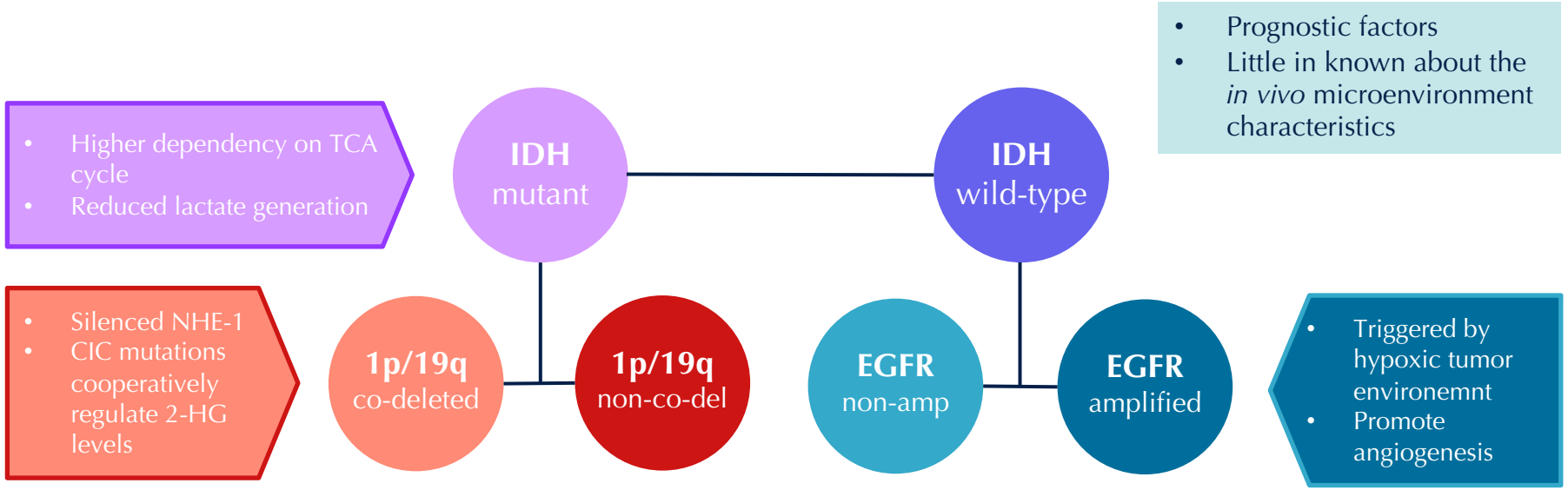

Patient demographics

Retrospective Study

Inclusion criteria

- Adult patient
- Pathologically confirmed glioma
- IDH status available
- Received CEST-EPI / CEST-SAGE-EPI scan

		2016 WHO Grading		
	All patients	**Grade II**	**Grade III**	**Grade IV**
No. of patients *(treatment naive / on treatment)*	159 (96/63)	42 (33/9)	38 (28/10)	79 (35/44)
Age *median [range]*	52 [19 - 90]	41 [22 - 90]	48.5 [21 - 70]	59 [19 - 83]
Sex *male / female*	101/58	24/18	24/14	53/26
IDH status *wild-type / mutant*	89/70	3/39	13/25	73/6
1p/19q status *in IDH mutant non-codeleted / codeleted / NA*	35/29/6	16/20/3	15/9/1	4/0/2
EGFR status in IDH wild-type wild-type / amplified / NA	42/40/7	2/1/0	9/3/1	31/36/6

Clinical validation: differentiating glioma genotypes

Acidity

Mutant ◀ Wild-type

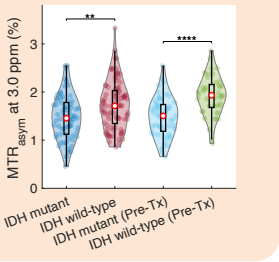

Hypoxia

Mutant ◀ Wild-type

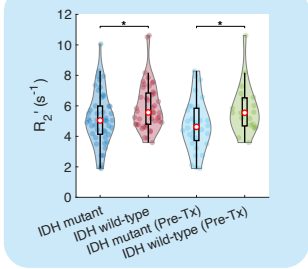

Acidity + Hypoxia

Mutant ◀ Wild-type

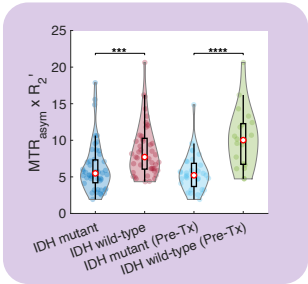

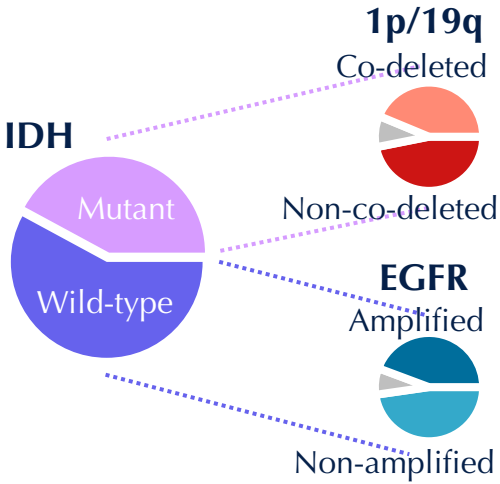

Acidity

Co-del ◀ Non-co-del

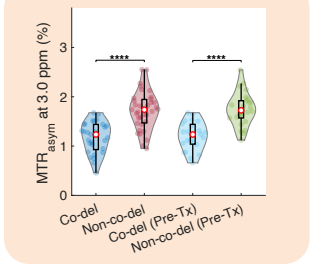

Hypoxia

Co-del ≈ Non-co-del

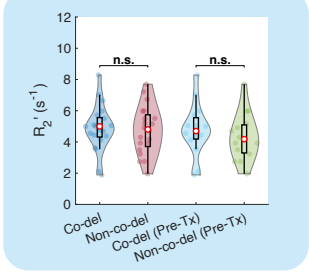

Amplified ≈ Non-amp

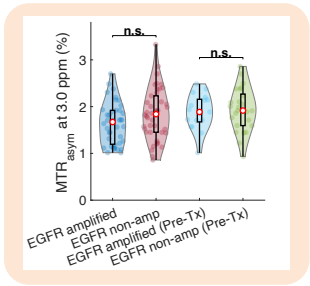

Amplified ▶ Non-amp

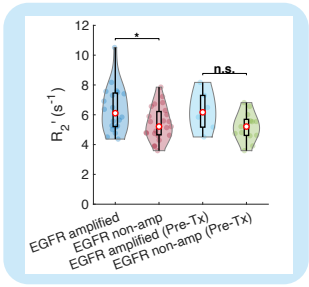

Yao J et al., Neuro-Oncology, 2019
Yao J et al., Cancers, 2022

Clinical validation: differentiating glioma genotypes

ROC analysis (treatment naïve patients N = 96)

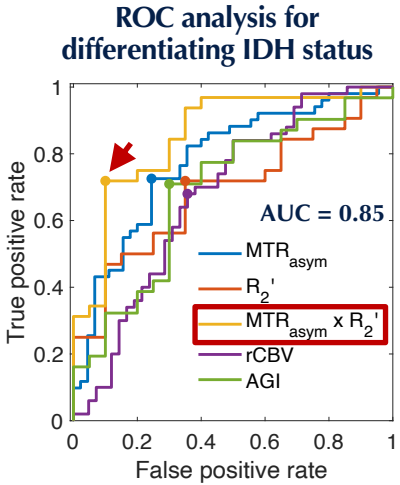

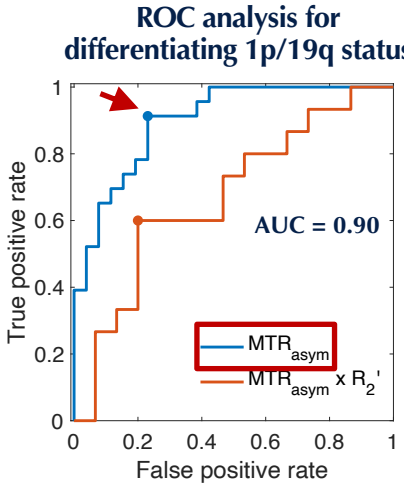

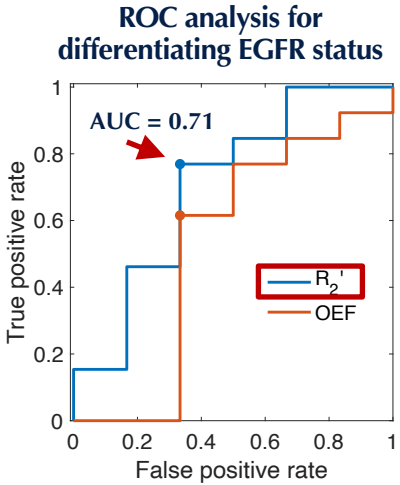

Yao J et al., Cancers, 2022

Clinical validation: differentiating glioma genotypes

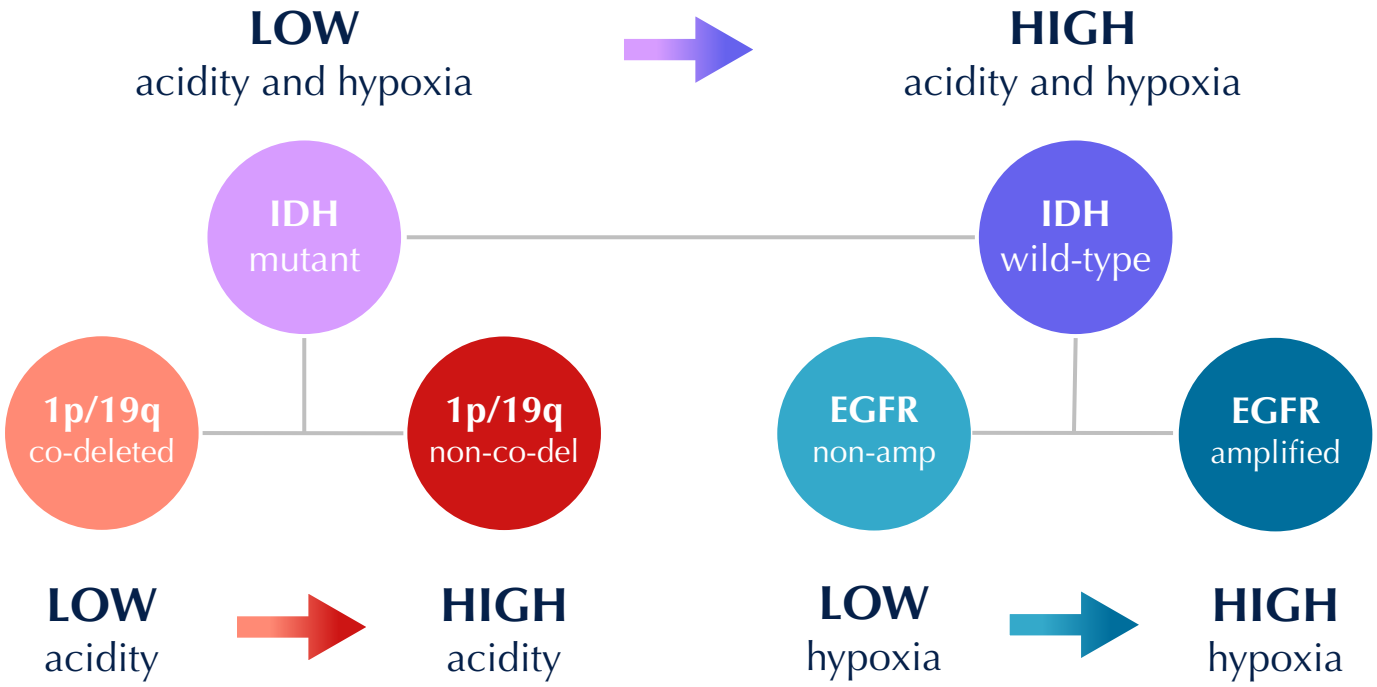

Yao J et al., Cancers, 2022

Clinical validation of pH- and oxygen-sensitive MRI

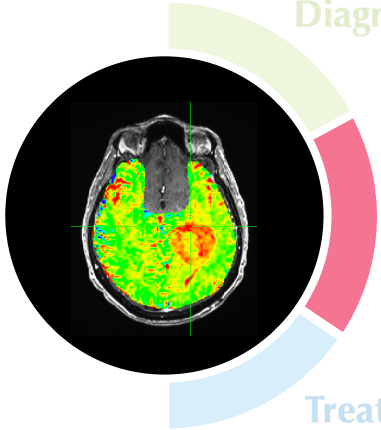

Diagnostic biomarker

Does the biomarker predict glioma genotypes?

Prognostic biomarker

Does the biomarker predict patient survival?

Treatment efficacy biomarker

Does the biomarker predict patient outcome?

Clinical validation: predicting patient survival

Overall survival

Cox Proportional-Hazards Model Analysis

- Univariate
- Multivariate with age, treatment status, and IDH status as covariates

Characteristics	OS (Univariate)			OS (Multivariate)		
	p-value	HR	HR [CI]	*p*-value	HR	HR [CI]
Age	**0.0002**	1.035	1.017 - 1.054		Covariate	
Treatment status	**< 0.0001**	3.748	2.250 - 6.241		Covariate	
IDH status	**< 0.0001**	0.093	0.042 - 0.206		Covariate	
MTR_{asym} at 3.0 ppm	0.2280	1.360	0.825 - 2.242	0.5474	1.1841	0.683 - 2.053
R_2'	**0.0002**	1.440	1.188 - 1.746	**0.0445**	1.2703	1.006 - 1.604
MTR_{asym} x R_2'	**0.0008**	1.140	1.056 - 1.231	**0.0019**	1.1655	1.058 - 1.284
CET+NET volume	**< 0.0001**	1.007	1.003 - 1.010	0.1526	1.0027	0.999 - 1.006
Acidic volume	**0.0003**	1.020	1.009 - 1.031	0.0931	1.0103	0.998 - 1.023
Acidic volume fraction	**0.0410**	1.021	1.001 - 1.041	0.3563	1.0098	0.989 - 1.031

Yao J et al., Cancers, 2022

Clinical validation: predicting patient survival

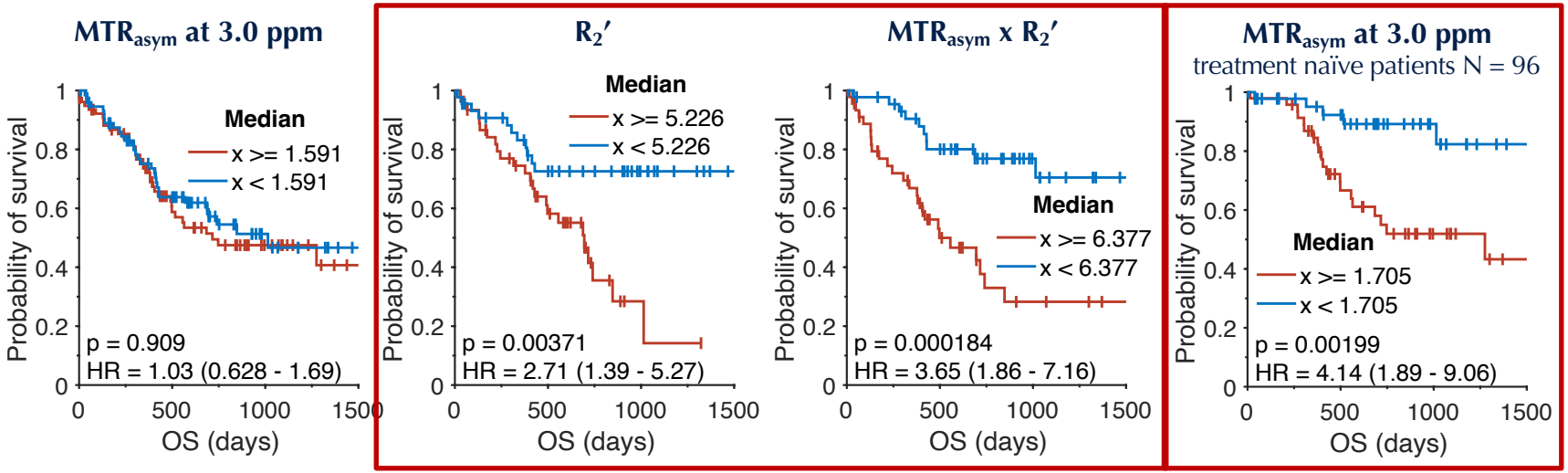

- **Tumor acidity and hypoxia** measured using pH- and oxygen-sensitive MRI are **significant prognostic factors** in glioma.
- Patients with more acidic and hypoxic tumors have significantly shorter survival.

Yao J et al., Cancers, 2022

Clinical validation of pH- and oxygen-sensitive MRI

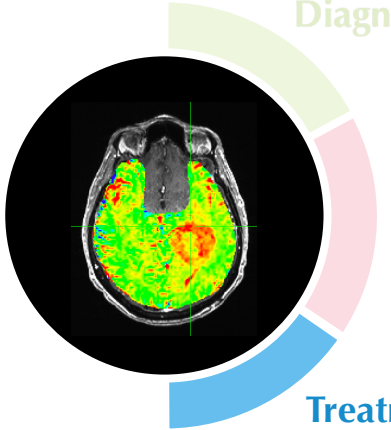

Diagnostic biomarker — Does the biomarker predict glioma genotypes?

Prognostic biomarker — Does the biomarker predict patient survival?

Treatment efficacy biomarker — Does the biomarker predict patient outcome?

Clinical validation: predicting treatment response

EGFR inhibitor

- Target oncogene-driven glucose metabolism

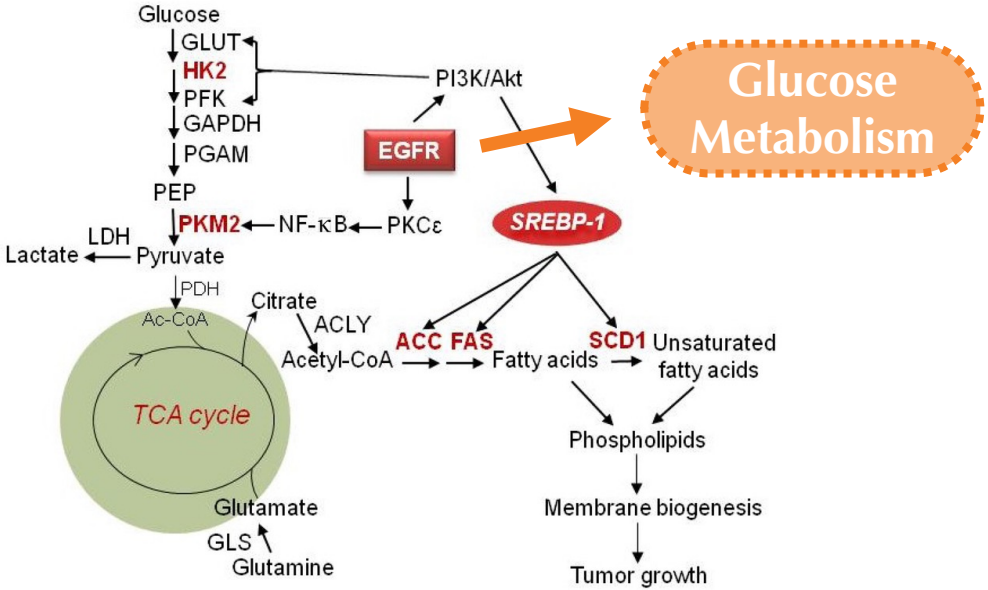

Ru P et al., 2013

Clinical validation: predicting treatment response

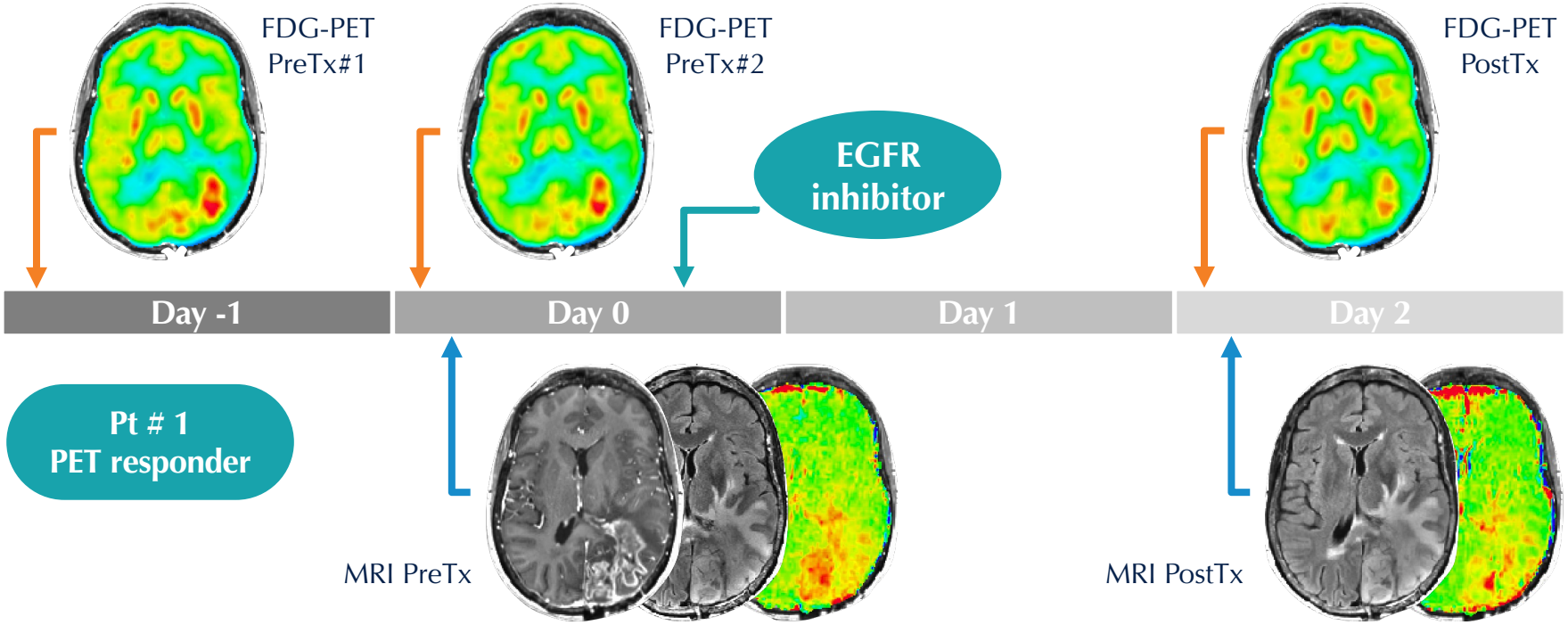

Clinical validation: predicting treatment response

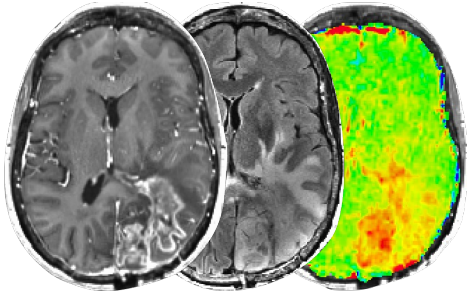

EGFR inhibitor

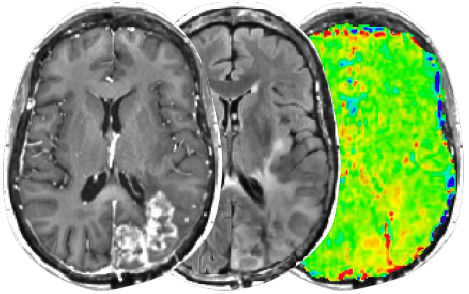

Pre-Tx | Post-Tx | One month

Pt # 1
PET responder

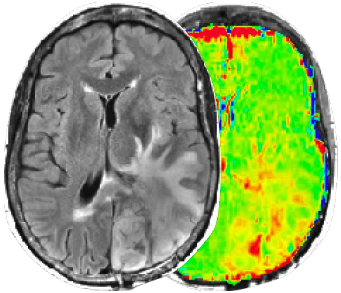

Clinical validation: predicting treatment response

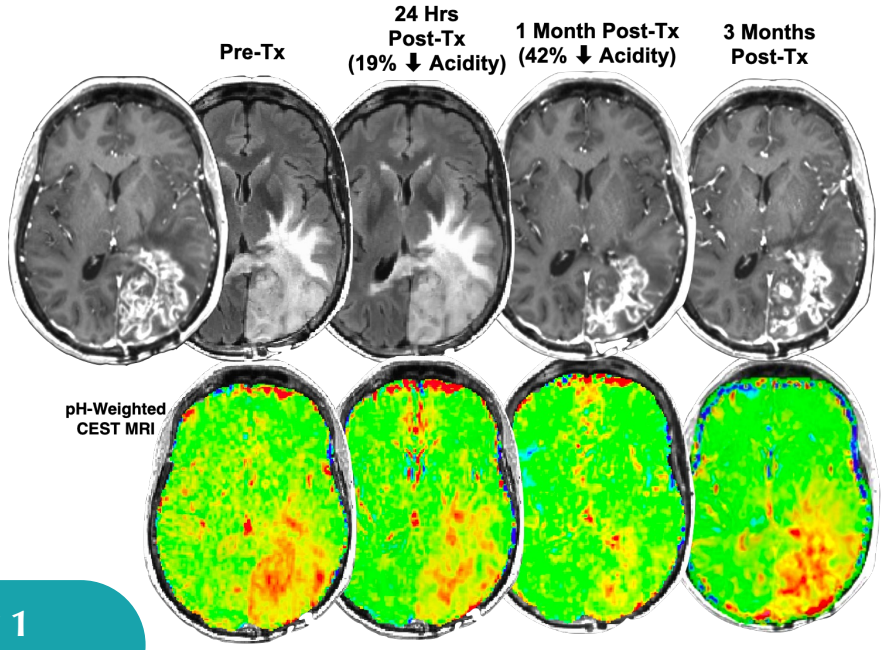

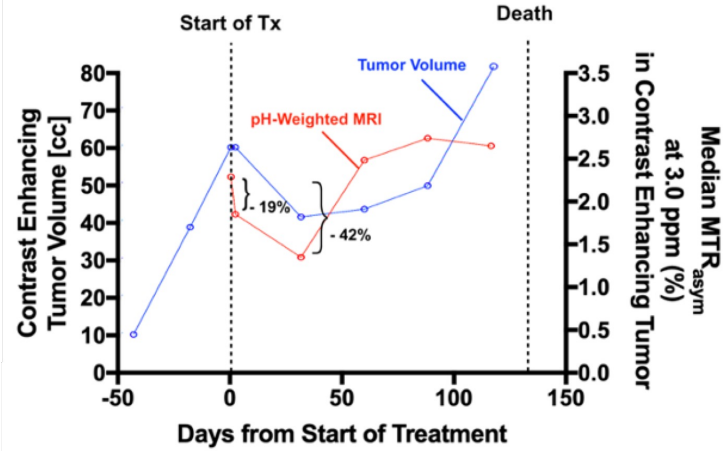

Pt # 1
PET responder

Clinical validation: predicting treatment response

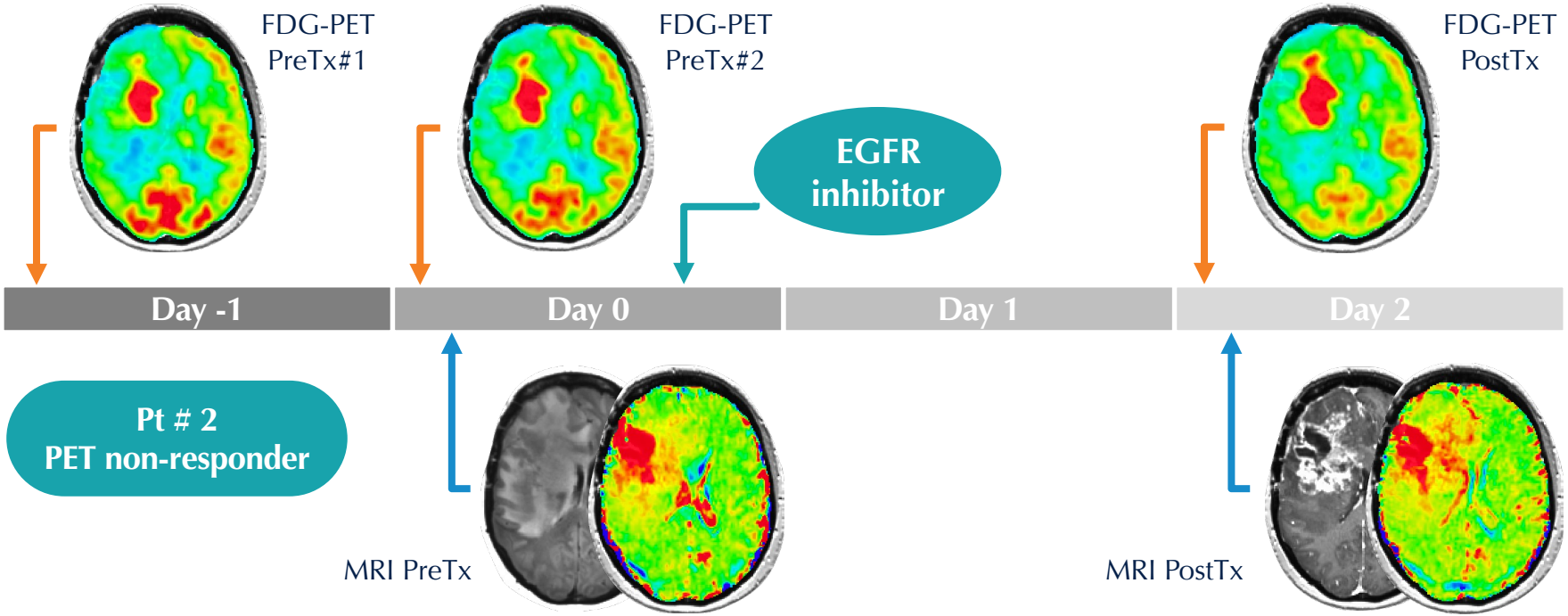

Clinical validation: predicting treatment response

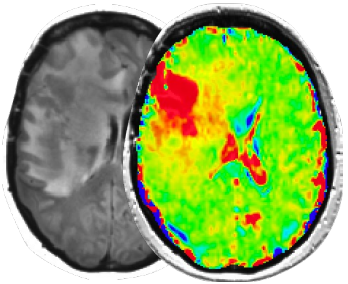

EGFR inhibitor

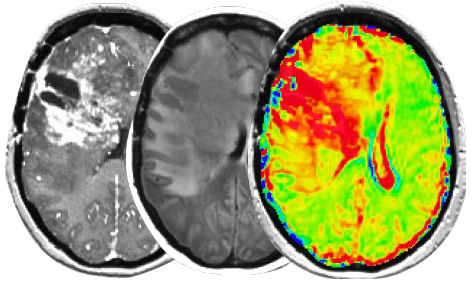

Pre-Tx | Post-Tx | One month

Pt # 2
PET non-responder

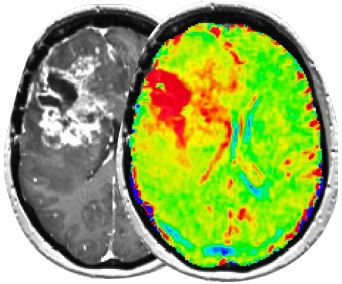

Clinical validation: predicting treatment response

- Baseline scan (Day 0)
- Post-Tx scan (Day 2)
- **FDG-PET measurements correlate with CEST measurements**

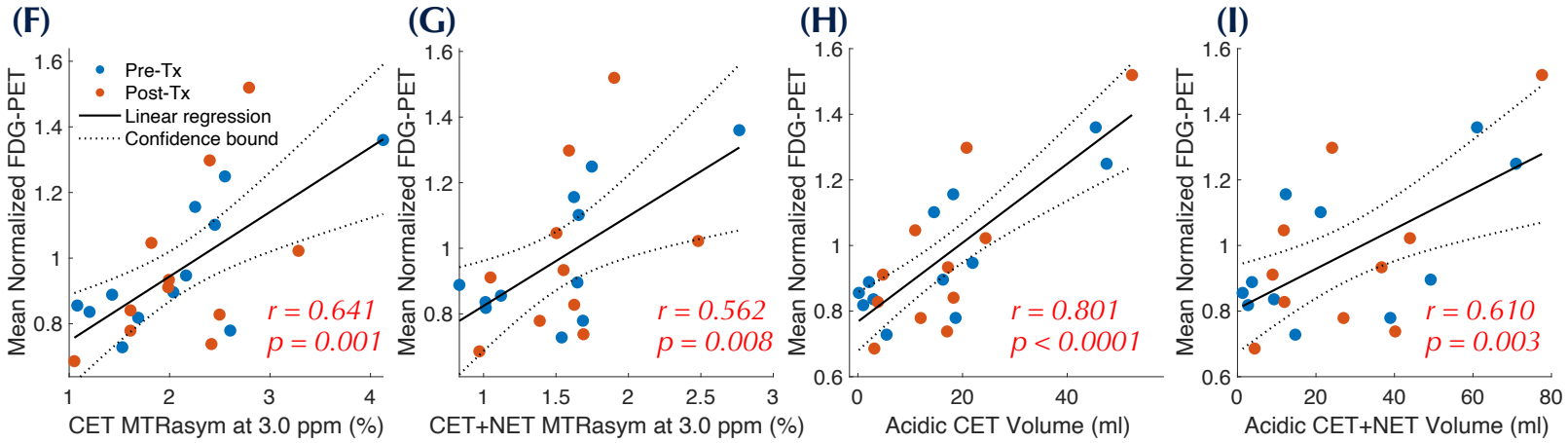

Clinical validation: predicting treatment response

	PFS (Univariate)			PFS (Multivariate)		
Characteristic	***p*-value**	**z-score**	**HR**	***p*-value**	**z-score**	**HR**
Volume						
Baseline	0.42	0.81	1.00 (0.98-1.02)	0.39	0.87	1.01 (0.99-1.02)
Normalized FDG						
Baseline	0.53	0.64	2.43 (0.16-37.32)	0.57	0.57	2.16 (0.15-31.39)
Post-Tx	0.33	0.98	4.12 (0.24-70.64)	0.38	0.87	3.48 (0.21-57.08)
Change	0.33	0.99	1.05 (0.95-1.17)	0.29	1.07	1.06 (0.95-1.18)
MTR_{asym} at 3.0 ppm						
Baseline	0.77	-0.29	0.85 (0.28-2.56)	0.67	-0.42	0.78 (0.24-2.53)
Post-Tx	**0.02**	2.39	12.93 (1.58-105.69)	**0.02**	2.35	13.38 (1.54-115.92)
Change	0.06	1.85	1.02 (1.00 1.05)	**0.04**	2.01	1.03 (1.01-1.06)
Acidic CET+NET Volume						
Baseline	0.73	0.34	1.01 (0.98-1.04)	0.80	0.26	1.00 (0.97-1.04)
Post-Tx	**0.02**	2.32	1.07 (1.01-1.14)	**0.02**	2.37	1.08 (1.01-1.14)
Change	0.12	1.56	1.01 (1.00-1.01)	0.10	1.67	1.01 (1.00-1.01)

- Post treatment CEST contrast and change in CEST contrast are predictive of patient outcome

Clinical validation: predicting treatment response

Decrease in Glycolytic Index (25%, 4 of 12) → Significant Increase in PFS (*HR=0.4, P=0.0467*) and OS (*HR=0.3, P=0.0192*)

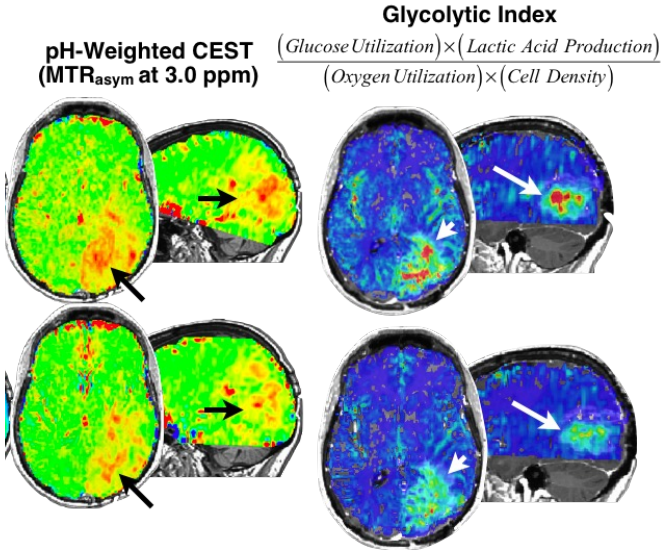

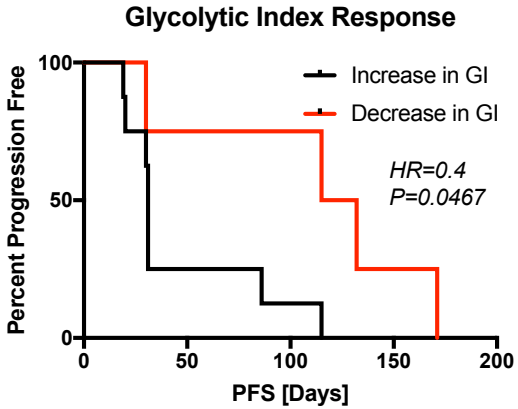

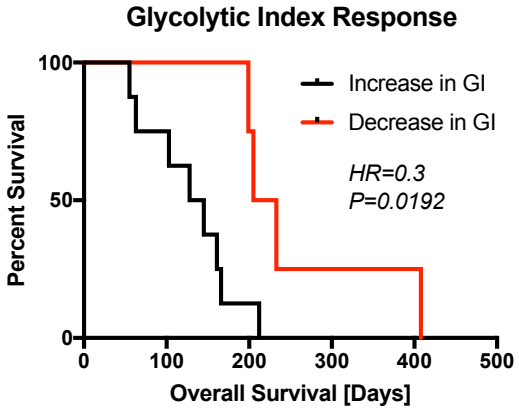

Outline

CEST

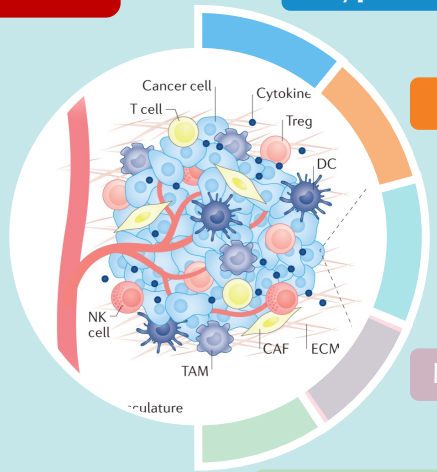

Hypoxia

Acidosis

Ion homeostasis

Neo-vasculature

Immune modulation

Glioma microenvironment

QSM

Brain iron imaging of subcortical nuclei in HD

Huntington's disease

Ongoing projects

1. Tumor associated macrophage imaging using ferumoxytol MRI
2. Understanding the role of cerebellum in HD

Iron imaging: Susceptibility MRI

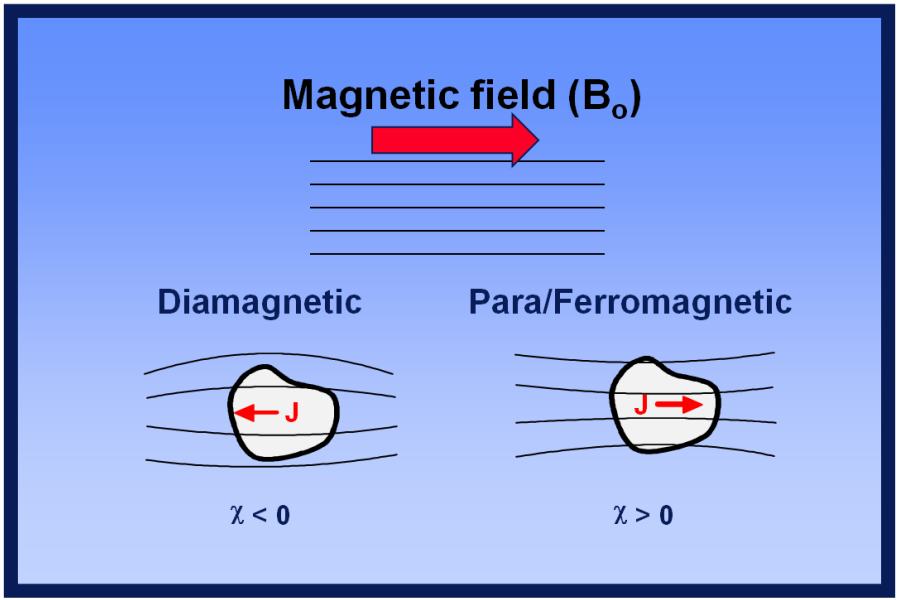

$$J = \chi B_0$$

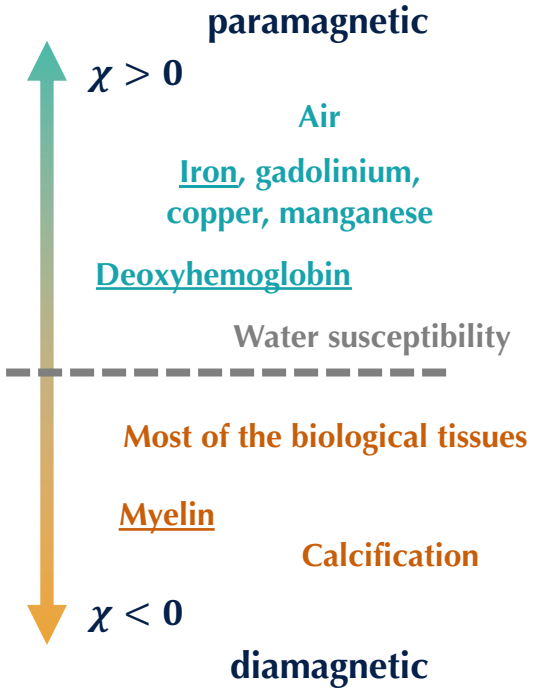

Iron imaging: Susceptibility MRI

Susceptibility-weighted imaging

Quantitative susceptibility mapping

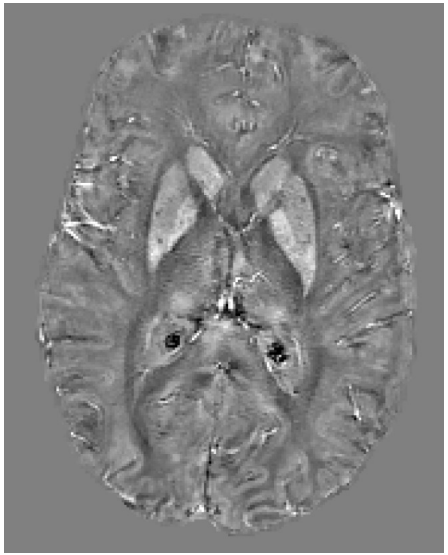

paramagnetic

$\chi > 0$

Air

Iron, gadolinium, copper, manganese

Deoxyhemoglobin

Water susceptibility

Most of the biological tissues

Myelin

Calcification

$\chi < 0$

diamagnetic

Barnes J et al., Magn Reson Imaging Clin N Am, 2010

QSM: Iron imaging biomarker

Phantom validation

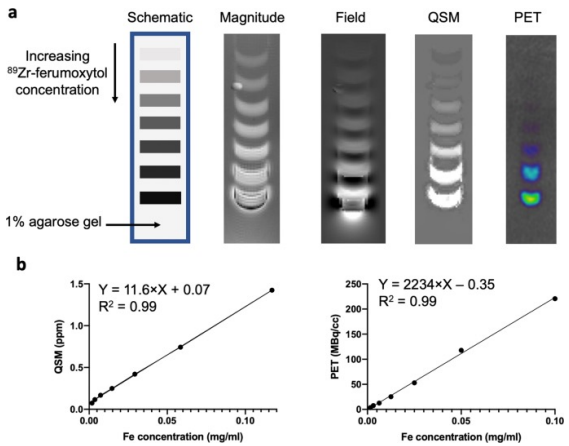

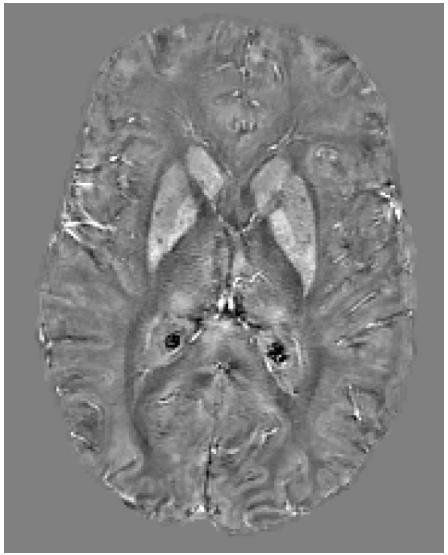

paramagnetic

$\chi > 0$

Air

Iron, gadolinium, copper, manganese

Deoxyhemoglobin

Water susceptibility

Most of the biological tissues

Myelin

Calcification

$\chi < 0$

diamagnetic

Deh K et al., Sci Rep, 2020

QSM: Iron imaging biomarker

Tissue validation

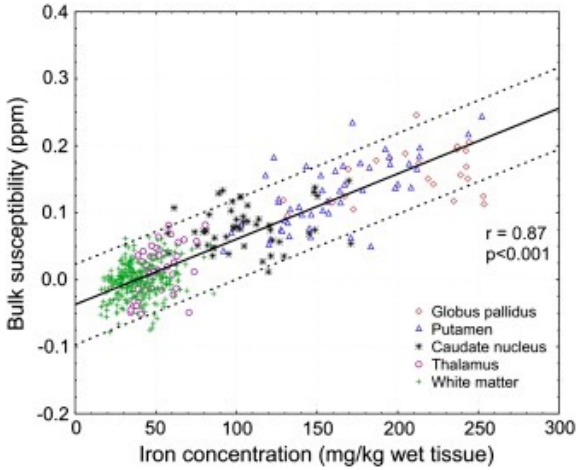

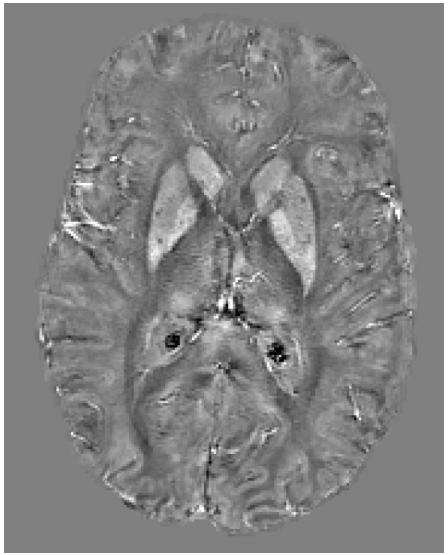

paramagnetic

$\chi > 0$

Air

Iron, gadolinium, copper, manganese

Deoxyhemoglobin

Water susceptibility

Most of the biological tissues

Myelin

Calcification

$\chi < 0$

diamagnetic

Lankammer C et al., NeuroImage, 2012

QSM: Iron imaging biomarker for neurodegenerative diseases

Alzheimer's Disease

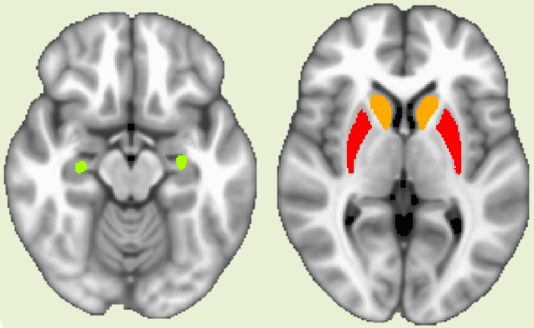

Parkinson's Disease

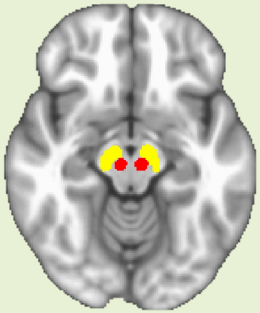

Huntington's Disease

Abnormal iron deposition in the subcortical brain regions in neurodegenerative diseases.

Huntington's disease

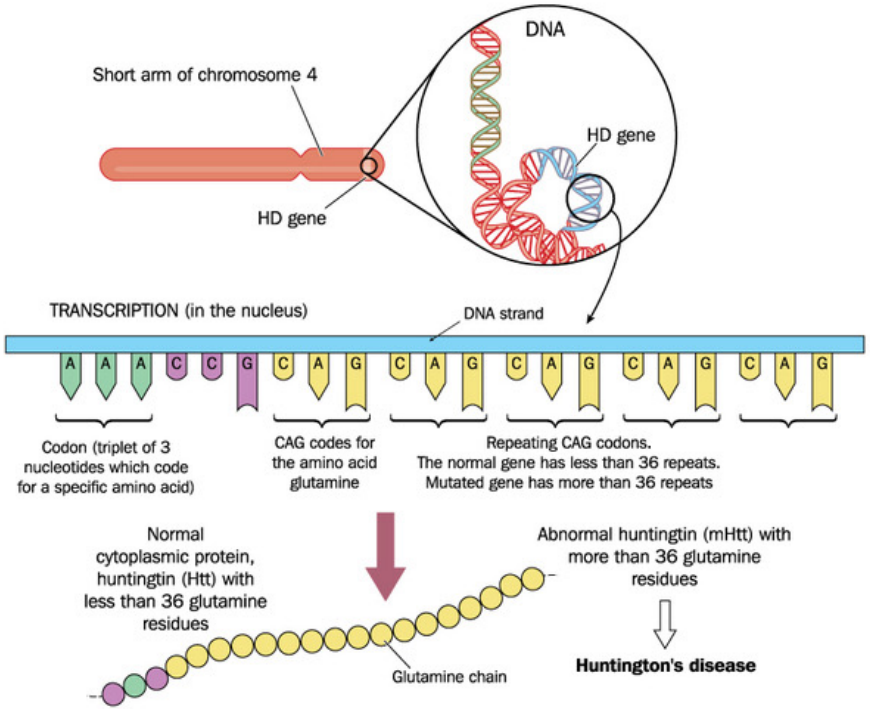

- Rare autosomal dominant disorder
- Huntingtin (HTT) gene mutation
  - CAG repeat length > 36

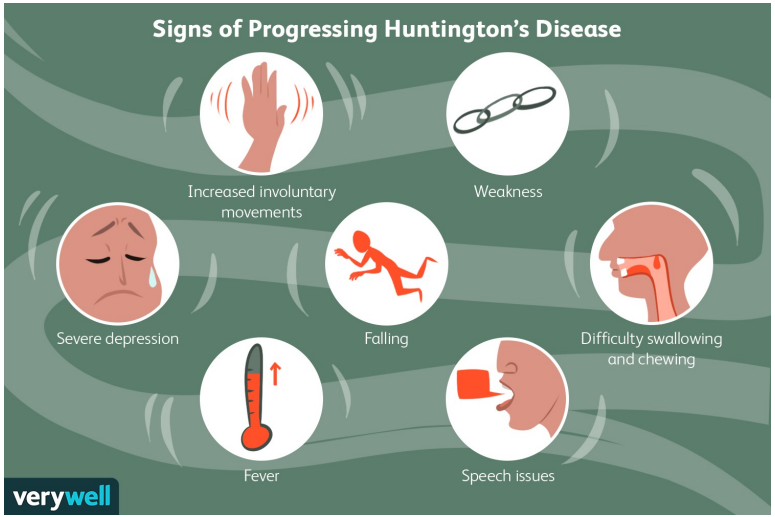

medlineplus.gov

Huntington's disease

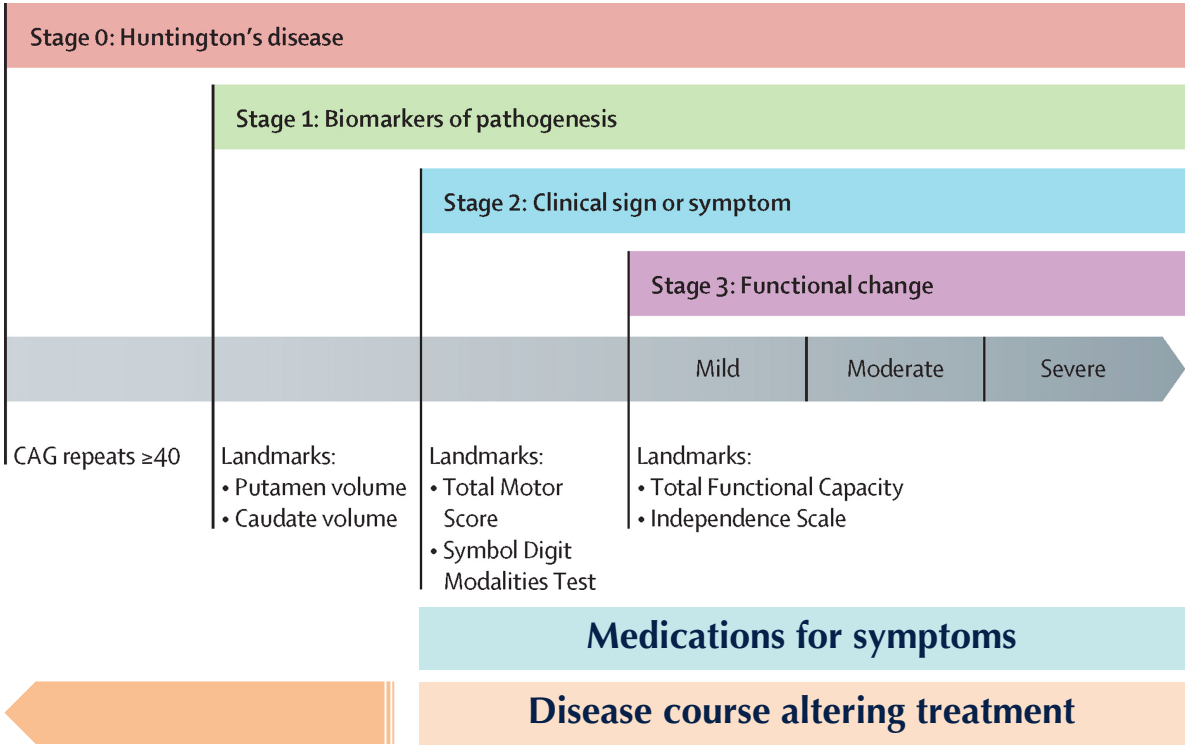

We need a **robust and quantitative method** to **monitor disease progression** and assess treatment efficacy before symptom onset.

Tabrizi SJ et al. 2022

Characterizing HD with advanced MRI

Characterize the **iron dysregulation** and **microstructural alteration** in subcortical brain regions with HD progression, using 7T MRI.

Quantitative susceptibility mapping (QSM)

Sensitive to iron deposition

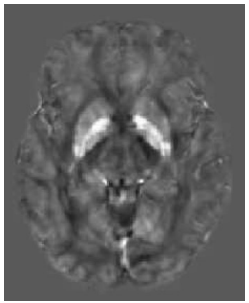

Diffusion Tensor Imaging

Fractional anisotropy (FA)
Mean diffusivity (MD)

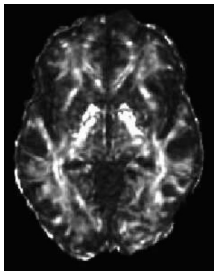

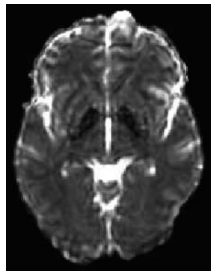

Study population

	Healthy Controls	All HD	PM Far From Onset (YTO > 15yr)	PM Near Onset (YTO < 15yr)	Manifest HD
Number	33	35	6	8	21
Sex (male/female)	16/17	15/20	3/3	2/6	10/11
Age (year)	43.9±12.2	44.7±12.8	36.3±10.7	39.3±11.8	49.1±12.1
CAG Repeat	N/A	42.3±2.8	40.7±1.6	43.1±2.3	42.5±3.1
CAPS	N/A	0.8±0.3	0.6±0.1	0.8±0.1	0.9±0.3
Estimated Year To Onset	N/A	8.7±12.2	23.5±5.7	9.6±5.2	N/A
TMS (total motor score)	N/A	11.4±10.1	2.0±2.3	3.0±2.5	17.3±8.8
TFC (total functional capacity)	N/A	12.3±1.5	13.0±0.0	12.5±0.9	12.0±1.8
DCL (diagnosis confidence level)	N/A	1.8±1.3	0.7±0.8	0.6±0.7	2.6±1.0

Imaging methods – iron imaging

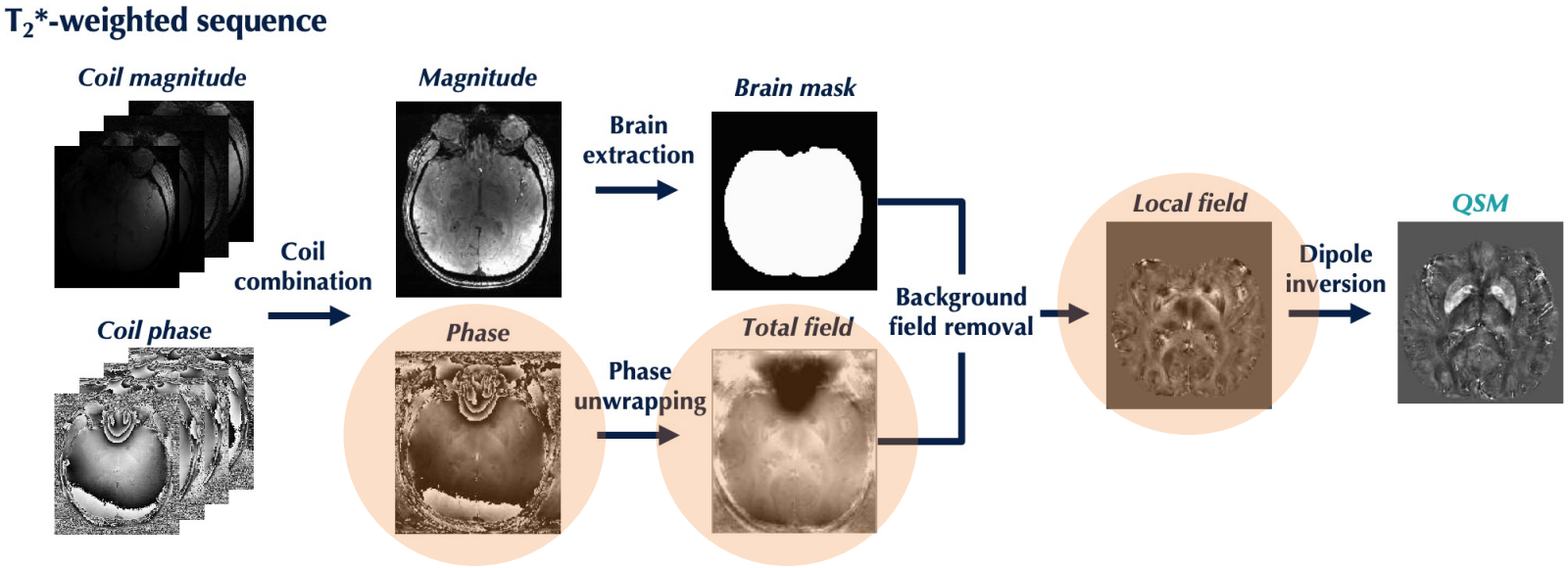

Imaging methods – microstructural imaging

Raw DTI images

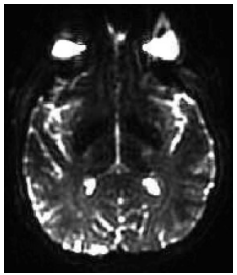

Pre-processing

Distortion correction, eddy current correction, etc.

Corrected DTI images

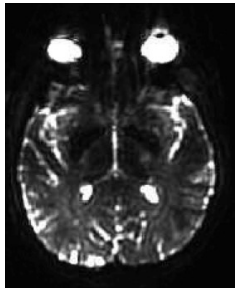

DTI fitting

FA

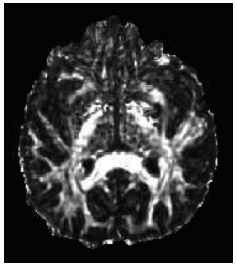

MD

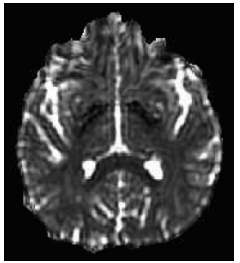

- Degree of directionality of water diffusion
- Axon and myelin integrity

- Overall diffusivity
- Cell density, edema, tissue microstructure

Subcortical brain regions

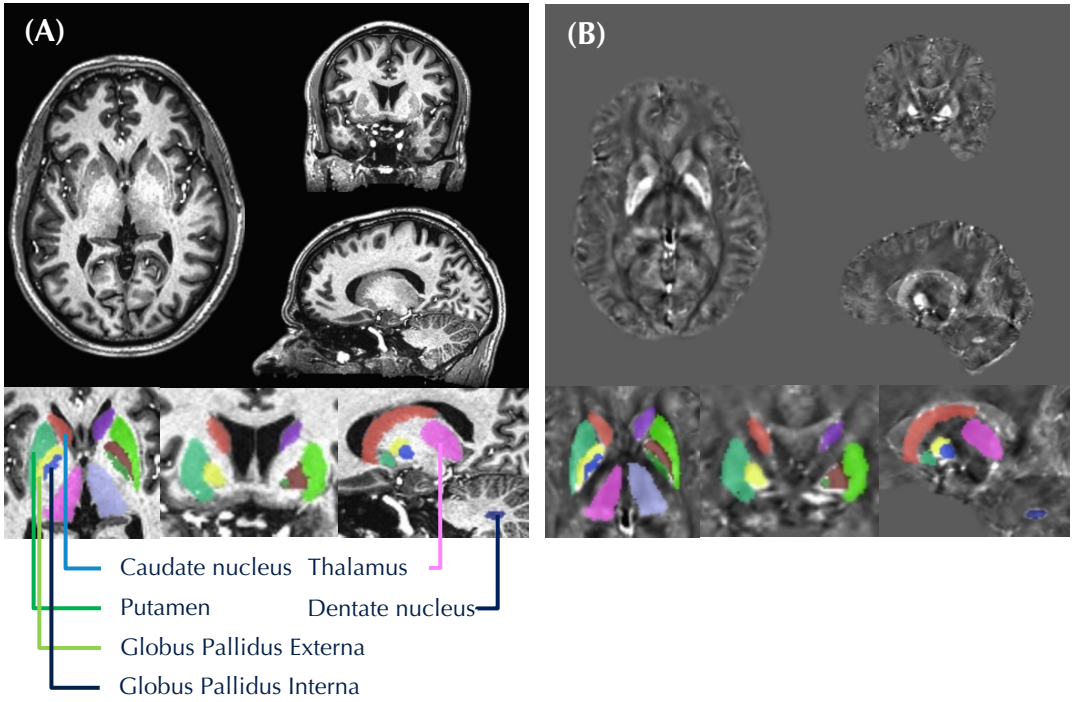

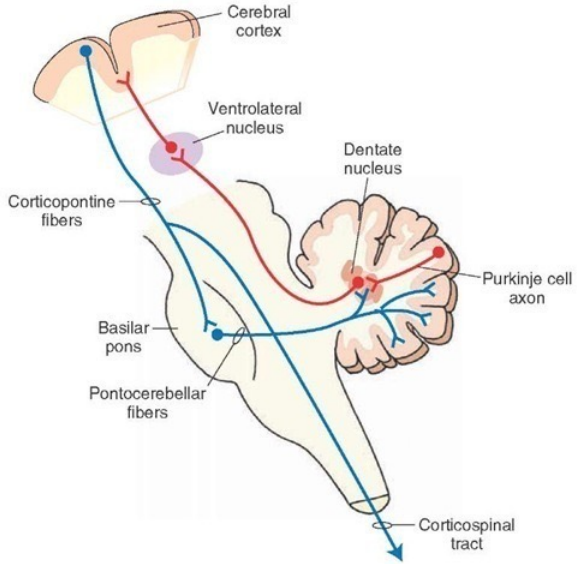

Cross-sectional comparisons of subcortical nuclei susceptibility & volume

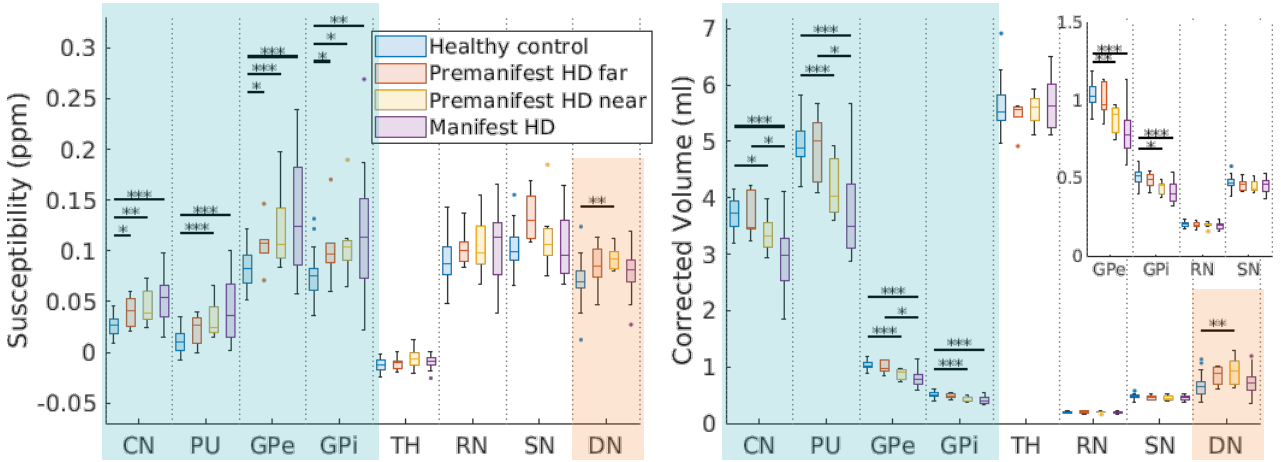

Iron deposition precedes volume changes.

Transient increases of volume and iron in the **dentate nucleus** of premanifest HD subjects suggest a new **early biomarker**.

Cross-sectional comparisons of subcortical nuclei FA & MD

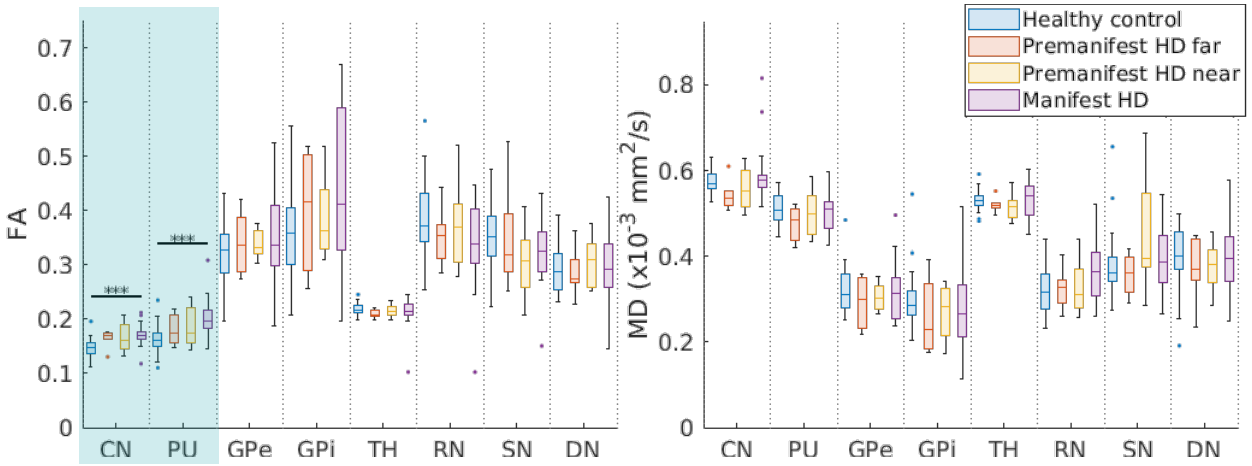

Striatum FA is **elevated** in HD.

Voxel-wise comparisons of susceptibility and FA

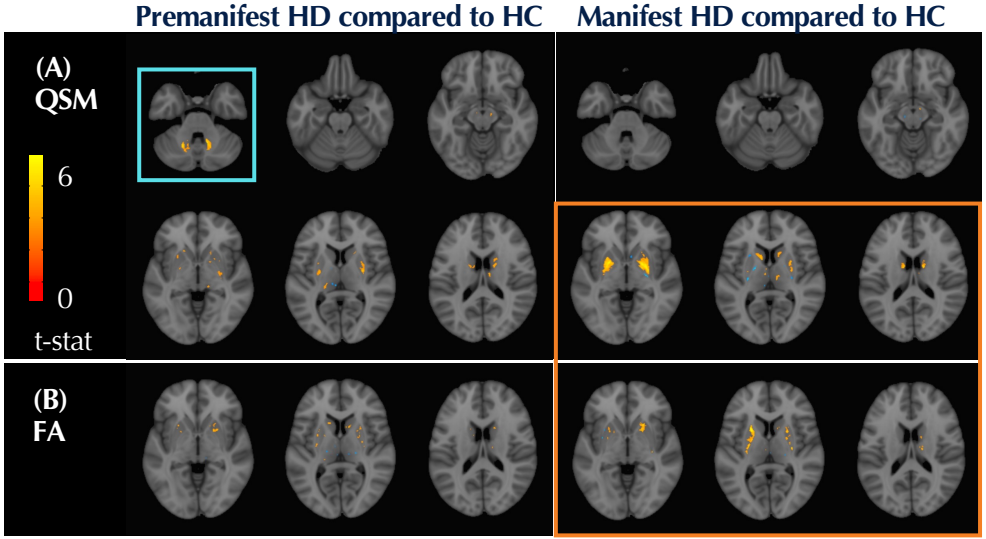

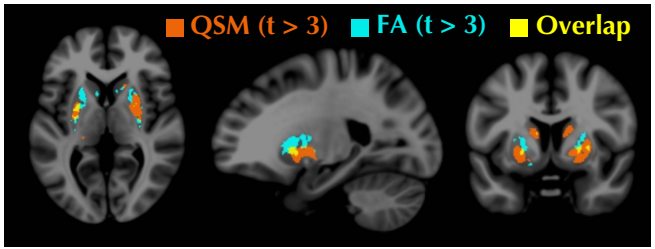

Putamen

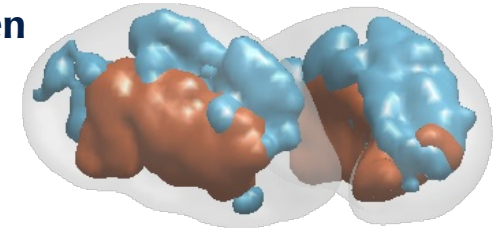

Elevated susceptibility and FA affect **different subregions of striatum** in HD.

Longitudinal analysis and correlation between susceptibility and volume

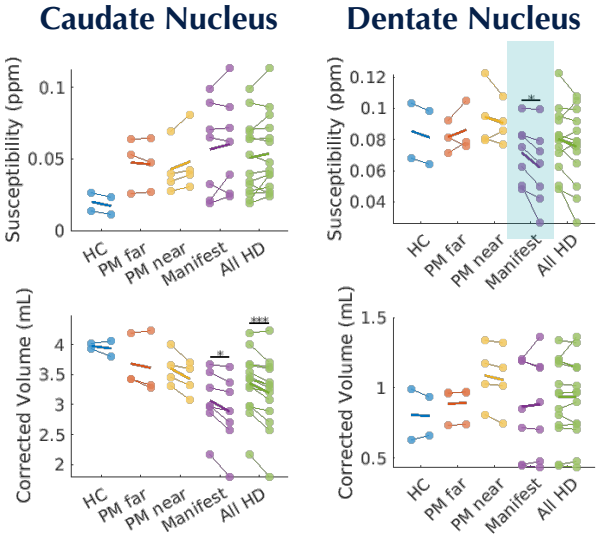

Iron deposition in dentate nucleus may follow **non-monotonic changes** as HD progress.

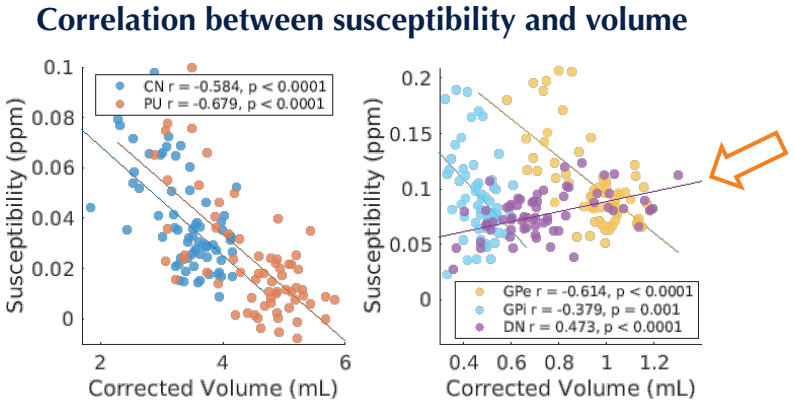

Iron deposition **correlates positively** with volume in **dentate nucleus**, potentially indicative of a previously less understood mechanism of HD pathogenesis.

Correlation with clinical assessments

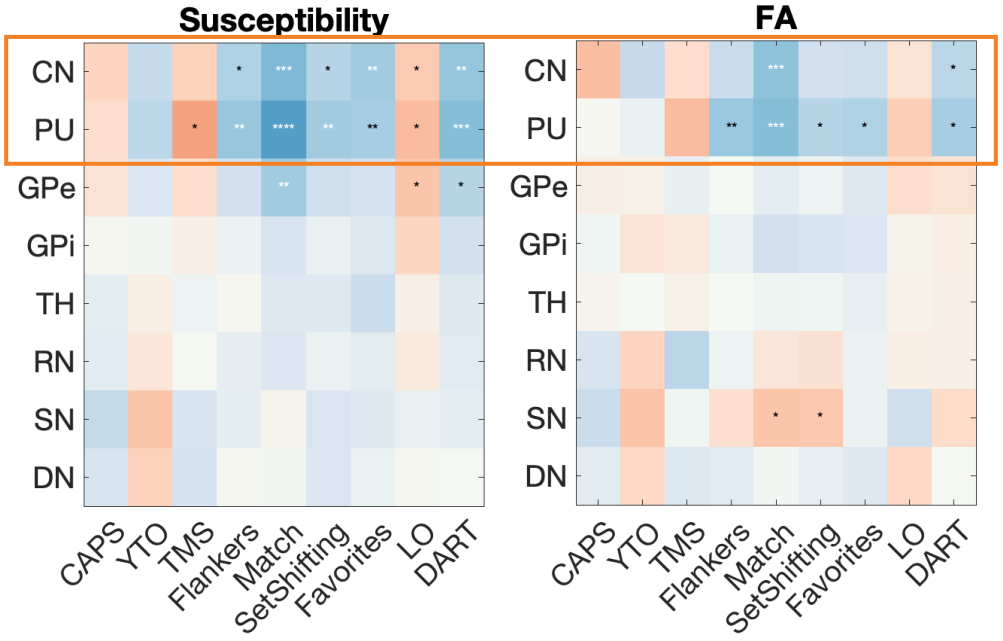

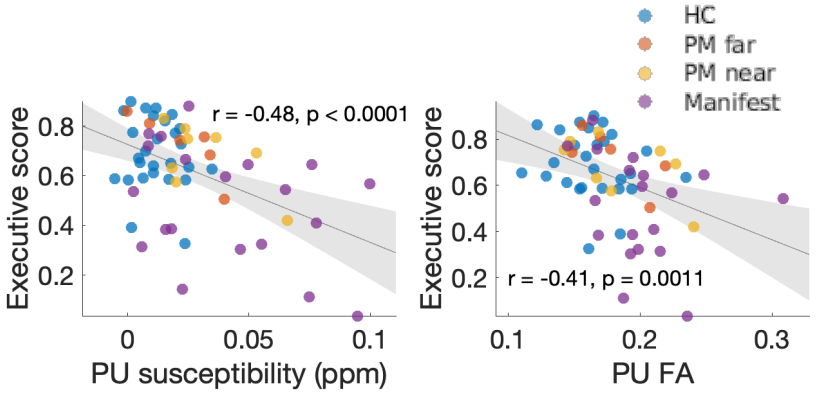

Increased caudate and putamen susceptibility/FA correlates with cognitive decline, showing the **strongest correlation with processing speed**.

Ongoing projects

Characterization of cerebellum in pre-manifest HD using multimodal MRI

- Validate **QSM as an early imaging biomarker** of HD at clinical field strength (3T)
- Elucidate the role of cerebellum in HD disease progression: **compensatory or pathologic**?

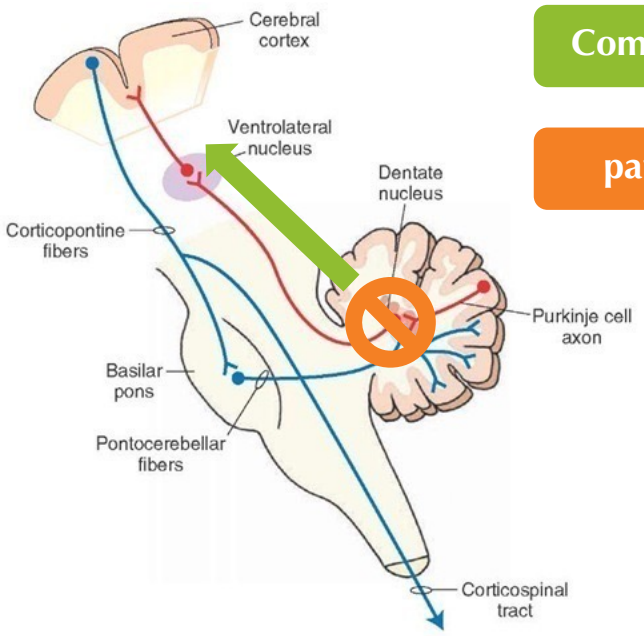

Compensatory ?

pathologic ?

Tereshchenko AV et al., Neurology, 2020

Ongoing projects

Tumor associated macrophage (TAM) imaging using QSM

Ferumoxytol-enhanced MRI
- Evaluate response to immune modulating therapies in glioma patients
- Develop phenotype-specific imaging biomarkers of TAMs

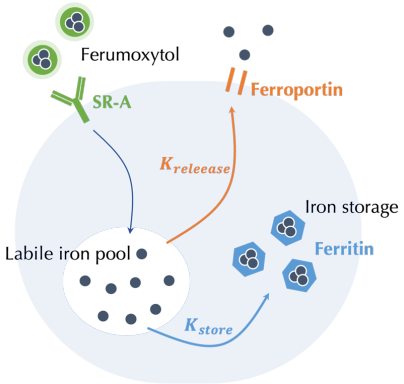

M1: iron-storing pro-inflammation

M2: iron-recycling pro-tumor

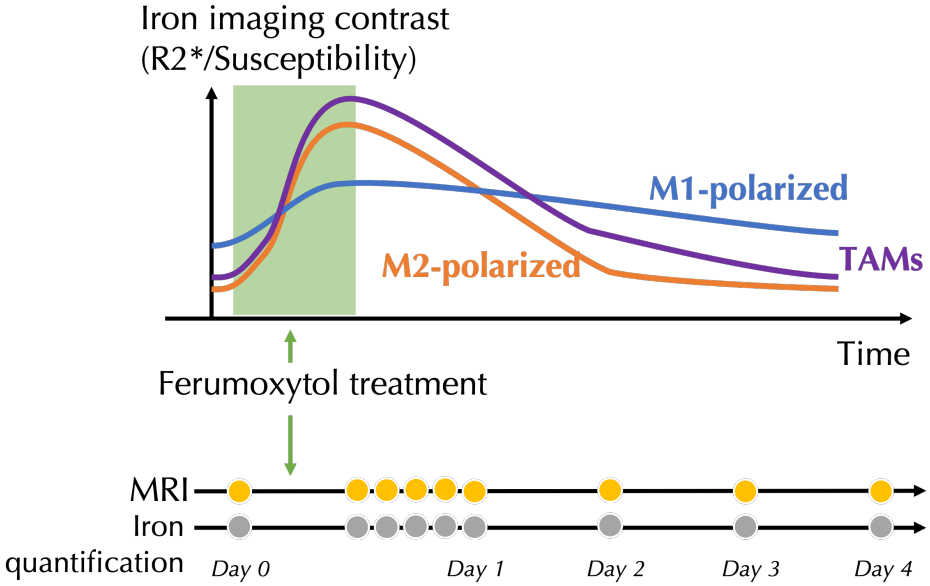

Brain Tumor Imaging Lab

Dr. Benjamin Ellingson
Catalina Raymond
Dr. Chencai Wang
Talia Oughourlian
Nicholas Cho
Dr. Robert Harris
Dr. Ararat Chakhoyan
Dr. Akifumi Hagiwara
Dr. Hiroyuki Tatekawa
Dr. Kunal Patel
Dr. Francesco Sanvito

UCLA Scientists and Clinicians

Dr. Timothy Cloughesy
Dr. David Nathanson
Dr. Noriko Salamon
Dr. Holden Wu
Dr. Denise Aberle
Dr. Whitney Pope
Dr. Albert Lai
Dr. Phioanh L. Nghiemphu
Dr. Linda Liau
Dr. Kim-Lien Nguyen
Dr. Robert Prins
Dr. Neil Harris

Lupo Lab

Dr. Melanie Morrison
Angela Jakary
Jacob Ellison
Paul Rowley
Ozan Genc
Dr. Eason Chen
Sivakami Avadiappan

Larson Lab

Dr. Abhejit Rajagopal
Dr. Xiaoxi Liu
Nikhil Deveshwar
Sule Sahin
Fei Tan
Avantika Sinha
Anna Bennett
Dr. Elizabeth Smith
Dr. Nick Dwork
Dr. Jessica Scholey
Dr. Andrew Leynes
Dr. Jeremy Gordon
Dr. Manuska Vaidya

UCSF/UCB Scientists and Clinicians

Dr. Yan Li
Dr. Duan Xu
Dr. Joseph Vu
Dr. Eduardo Caverzasi
Dr. Christopher Hess
Dr. Javier Villanueva-Meyer
Dr. Henry Roland

Outline

CEST

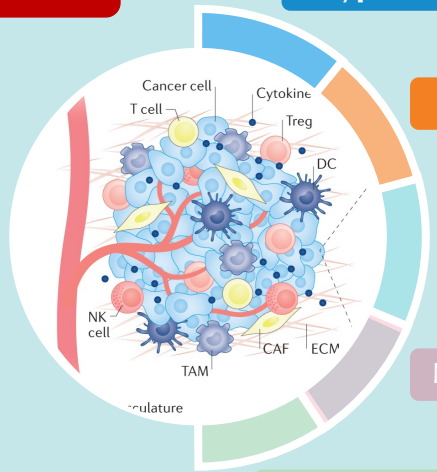

Hypoxia

Acidosis

Ion homeostasis

Neo-vasculature

Immune modulation

Glioma microenvironment

QSM

Brain iron imaging of subcortical nuclei in HD

Huntington's disease

Ongoing projects

1. Tumor associated macrophage imaging using ferumoxytol MRI
2. Understanding the role of cerebellum in HD